Novel gold nanoparticles of drought tolerance enabler GYY4137

UNIVERSITY *of the*
WESTERN CAPE

By

Ntombikayise Binase

UNIVERSITY of the
WESTERN CAPE

A mini-dissertation submitted in partial fulfilment of the requirements for the degree of Magister Scientiae in Nanoscience

Faculty of Natural Science

University of the Western Cape,

Cape Town, South Africa

Supervisor: Prof.Ndiko N. Ludidi

Co-supervisor: Prof. Martin O. Onani

https://etd.uwc.ac.za

Novel gold nanoparticles of drought tolerance enabler GYY4137

Ntombikayise Binase

Keywords

Nanotechnology

Agriculture

Morpholin-4-ium 4-methoxyphenyl (morpholino) phosphinodithioate (GYY4137)

Drought tolerance

Gold Nanoparticles

Poly ethylene glycol (PEG)

Chitosan

UNIVERSITY of the
WESTERN CAPE

https://etd.uwc.ac.za

Abstract

Novel gold nanoparticles of drought tolerance enabler GYY4137

MSc. Mini-dissertation, Biotechnology Department, University of the Western Cape

N. Binase

Different nanoparticles have the ability to improve plant tolerance to drought stress. In the study we report for the first time novel morpholin-4-ium 4-methoxyphenyl (morpholino) phosphinodithioate capped- gold nanoparticles (GYY4137-capped AuNPs). The GYY4137 is a slow releasing hydrogen sulfide (H_2S) donor. The GYY4137 AuNPs compared to preliminary experiments of L-serine and L-threonine gold nanoparticles. The nanoparticles were prepared using a simple reflux reduction method in a rolling boil flask at 80 ^{o}C. The uncapped GYY4137-AuNPs were relatively stable and had surface plasmon resonance at 562 nm compared to 524 nm and 560 nm of serine-AuNPs and threonine-AuNPs. The nanoparticles were capped with different concentrations (0.1-5 %) of water-soluble poly (ethylene) glycol (PEG) (M_{w300}) and 0.2% chitosan. The PEG did not fully encapsulate the gold nanoparticles, while the chitosan successfully produced positively charged gold nanoparticles. The formation of chitosan capped GYY4137-AuNPs were verified with UV-Visible spectroscopy (UV-Vis), High Resolution Transmission electron microscopy (HRTEM), Dynamic Light scattering (DLS) and the Zetasizer. The UV-Vis, HRTEM and STEM verified chitosan capped nanoparticles had a surface plasmon resonance peak at 560 nm, with icosahedral, tetrahedron and spherical shaped nanoparticles as the serine-AuNPs that absorb at 560 nm. The agglomerated threonine-AuNPs had a maximum absorbance peak at 524 nm. The chitosan GYY4137-AuNPs had hydrodynamic size of 347.9 nm and zeta potential of + 47 mV, while serine-AuNPs and threonine-AuNPs had hydrodynamic size of 110 nm, zeta potential of -2.9 mV and -230 mV respectively. The polydispersity index (PDI) of the chitosan capped gold nanoparticles was 0.357 compared to 0.406 of both the amino acid gold nanoparticles. The polydispersity index (PDI) showed that the nanoparticles were polydispersed nanoparticles with broad size range as confirmed by the HRTEM and STEM results/ of chitosan capped GYY4137-AuNPs. The sizes of the nanoparticles were 100 nm and 60 nm for GYY4137-AuNPs while the size serine-AuNPs were 60 nm. The gold

UNIVERSITY of the WESTERN CAPE

https://etd.uwc.ac.za

nanoparticles structural compositions were further confirmed by energy-dispersive X-ray spectrometry (EDX) and Attenuated total reflection infrared spectroscopy (ATR-IR). EDX results proved successful gold nanoparticles synthesis by presence of the element Au in all three nanoparticles and the chitosan GYY4137-AuNPs had 48. 56 wt. % of gold. The FTIR-ATR new bands formation shows that new chemical bonds are formed between the reducing agents, the precursor gold salt solution and capping agents. The shifts showed successful encapsulation with chitosan in GYY4137-AuNPs. The chitosan encapsulation improved surface charge and reactivity of the gold nanoparticles to improve delivery of the hydrogen sulfide donor GYY4137 for later applications to plants.

UNIVERSITY of the
WESTERN CAPE

https://etd.uwc.ac.za

Declaration

University of the Western Cape

Private Bag X17, Bellville 7535, South Africa

Telephone: ++27-21- 959 2255/959 2762Fax: ++27-21- 959 1268/2266

FACULTY OF NATURAL SCIENCE

Name: Ntombikayise Binase……

Student number: 3138504……

1. I hereby declare that I know what plagiarism entails, namely to use another's work and to present it as my own without attributing the sources in the correct way. (Refer to University Calendar part 1 for definition)
2. I know that plagiarism is a punishable offence because it constitutes theft.
3. I understand the plagiarism policy of the Faculty of Natural Science of the University of the Western Cape.
4. I declare therefore that all work presented by me is my own, and where I have made use of another's work, I have attributed the source in the correct way.

---------- 08-08-2019 ----------

Signature: Ntombikayise Binase Date

https://etd.uwc.ac.za

Dedications

I dedicate my MSc. Mini-dissertation to my first lady Tembisa Binase who has always been the pillar of my strength through all my hardships. She has always told me “Inkomo yobuthongo ayikho mntwanam” in our culture that means you will not gain anything by sleeping. She has loved, supported, brought great laughter in times of distress and nurtured me throughout my life. I give her this mini-dissertation to my show full appreciation. Not forgetting my paternal grandfather Mgqwashu (May his soul rest in peace) he always encouraged me to go as far as possible with education. He would say “Nosisi (my nickname) is right by going to school until she finishes all her education “with a great smile. Defending my never-ending education from my cousins.

UNIVERSITY of the
WESTERN CAPE

https://etd.uwc.ac.za

Acknowledgements

I would like to thank all:

- Firstly, the **only true living God** of **Twelve Apostles' Church in Christ (TACC)** for carrying me thus far. This has been a very long rough journey.
- Thank you to the **Department of Science and Technology (DST)** for funding me through the **National Nanoscience Teaching and Training Platform (NNTTP**) a great initiative to spread the word about this new technology in South Africa.
- **Ms Valencia Jamalie** and **Prof Dirk Knoesen** for their dedication to administration and making sure students finish their mini-dissertation on time.
- Thanks to both my supervisors **Prof. N. Ludidi** (Biotechnology) and **Prof. M. Onani** (Chemistry) for their academic support and guidance.
- Thanks to the lab mates from the **Nanomaterials and Organometallic Research Laboratory** for welcoming me and for their continued patience and support.
- **Dr. Ayabei Kiplagat**, for showing me the ropes in the lab and Ms Shonny Nkuna for helping me with my chemistry in the mini-dissertation
- I thank you Mr Lesch for helping with operation of ATR-FTIR and UV-Vis equipment in the department of chemistry, UWC.
- A special thanks to my wonderful father **Mr Mboneni Malothana** and husband Mr**. Sandisile Molosi** their support and for Godly encouragement when things were going west.

"I call it **RESEARCH** because we **SEARCH** for the unknown in hope for **SOLUTIONS**. All we can do is **HOPE** for a result." Another man's conclusion proves **potential** to lead to another man's **Discovery**.

UNIVERSITY of the
WESTERN CAPE

https://etd.uwc.ac.za

Publications and Conference Contributions

Binase, N., Ludidi, N., Onani, M. Synthesis and Characterization of H_2S donor AuNPs for Application into drought stressed cowpea, African Materials Research Society International Conference (AMRS), BITRI Gaborone, Botswana. 9 – 14th December 2017, **Poster presentation.**

UNIVERSITY of the
WESTERN CAPE

https://etd.uwc.ac.za

Table of Contents

Keywords ii

Abstract iii

Declaration v

Dedications vi

Acknowledgements vii

Publications and Conference Contributions viii

Abbreviations and symbols xii

List of Figures xiv

List of Tables xvi

Chapter 1 1

Chapter Overview 1

1. Introduction 1

1.1. Nanotechnology in biotechnology. 1

1.2. General use of nanomaterials in agriculture 2

1.2.1. Nanomaterials as fertilizers. 3

1.2.2. Nanomaterials as Biosensors. 5

1.2.3. The nanomaterials as plant protecting products. 7

1.3. Nanomaterials improve drought tolerance. 10

1.3.1. Inorganic nanomaterials improve plants drought tolerance. 10

1.3.2. Carbonaceous nanomaterials in drought tolerance. 11

1.4. The GYY4137 effect on drought stress. 12

1.5. Comparison of GYY4137 to NaHS. 12

1.6. Problem Statement 13

UNIVERSITY of the WESTERN CAPE

https://etd.uwc.ac.za

1.7. Research aims and objectives 13

1.8. References 14

Chapter 2 19

Literature review 19

Chapter Overview 19

2.1. History of gold nanoparticles. 19

2.2. General properties and applications of gold nanoparticles. 20

2.3. Studies of gold nanoparticles in agriculture 21

2.3. Description of PEG and chitosan. 23

2.5. References 25

Chapter 3 28

Chapter Overview 28

3. Method and Materials 28

3.1. Chemicals 28

3.2. GYY4137, serine and threonine AuNPs synthesis. 28

3.2.1. GYY4137 AuNPs capping with PEG and chitosan. 29

3.3. Characterization Of the gold nanoparticles. 29

3.3.1. Ultraviolet Visible (UV-Vis) spectroscopy 29

3.3.2. High resolution Transmission microscopy (HRTEM) analysis 30

3.3.3. Energy dispersive X-Ray Analysis (EDX) analysis. 31

3.3.4 Scanning Transmission Electron Microscopy (STEM with EDAX) 31

3.3.5. Attenuated Total Reflectance Fourier Transform Infrared spectroscopy (ATR-FTIR) analysis 32

3.3.6. Dynamic Light scattering and Zeta Potential 33

UNIVERSITY of the
WESTERN CAPE

https://etd.uwc.ac.za

3.4. References 35

Chapter 4 37

Chapter overview 37

4. Results and Discussion 37

4.1. The formation of GYY4137-AuNPs, serine-AuNPs and threonine-AuNPs. 37

4.3. Characterization of chitosan capped GYY4137-AuNPs. 42

4.3.1. Functional groups of chitosan capped GYY4137-AuNPs. 44

4.3.2. The hydrodynamic size and size distribution of chitosan capped GYY4137-AuNPs. 48

4.3.3. Surface charge (Z) of the chitosan capped GYY4137-AuNPs. 49

4.2.6. Morphology of chitosan capped-GYY4137–AuNPs. 50

4.2.8. Elemental mapping of chitosan capped GYY4137-AuNPs. 53

4.3. References 56

Chapter 5: Conclusions and Future Perspectives 59

5.1. Conclusions 59

5.2. Future Perspectives 59

Appendix 1: HRTEM structural shapes of chitosan capped GYY4137 nanoparticles 60

UNIVERSITY of the
WESTERN CAPE

https://etd.uwc.ac.za

Abbreviations and symbols

Ascorbate peroxidise	APX
Arabidopsis thaliana.	*A. thaliana*
Attenuated total reflection infrared spectroscopy	ATR-IR
Bacillus thuringiensis	Bt
Catalase	CAT
Chitosan	deacetylated chitin poly (D-glucosamine)
Degree of deacetylation	DDA
Dynamic Light and Scattering	DLS
Energy-dispersive X ray spectroscopy	EDS
Glutathione reductase	GR
Gold Nanoparticles	AuNPs
Hydrochloric acid	HCl
Hydrogen sulfide	H_2S
Infrared	IR
Micro molar	µM
microRNA	mRNAs
Milligrams per litre	mg L^{-1}
milli molar	mM
milli volts	mV
Morpholin-4-ium 4-methoxyphenyl (morpholino) phosphinodithioate	GYY4137
nanogram per litre	ng. L^{-1}
Nanometre	nm

UNIVERSITY of the
WESTERN CAPE

https://etd.uwc.ac.za

Nitric acid	HNO_3
Oxidised gold iron	Au^{3+}
Parts per million	ppm
Percent	%
Poly (ethylene) glycol	PEG
Reciprocal centimetre	cm^{-1}
Reduced gold	Au^{0}
Resolution transmission electron microscopy	HRTEM
Revolutions per minute	rpm
Sodium hydrosulfide	NaHS
Sodium tripolyphosphate	$Na_5O_{10}P_3$
Superoxide dismutase	SOD
Tetrachloroauric (III) acid	$HAuCl_4$
Ultraviolet-Visible Spectroscopy	UV-Vis
Weight percentage	wt. %

UNIVERSITY of the
WESTERN CAPE

https://etd.uwc.ac.za

List of Figures

Figure	Page
1: The applications of nanomaterial in agriculture	9
2: Chitosan and PEG structures	24
3: schematic diagram of double beam UV-Vis apparatus.	30
4: General layout of a HRTEM with EDAX.	31
5: A Schematic representation of ATR-FTIR.	33
6: GYY4137- AuNPs, serine-AuNPs and threonine-AuNPs solutions. (**a**) Uncapped GYY4137 AuNPs, **(b)** serine-AuNPs and**(c)**. threonine- AuNPs.	38
7: UV-Vis spectra of G YY4137-AuNPs compared to amino acid AuNPs. (Purple) GYY4137-AuNPs (Blue) threonine-AuNPs and (Green) Serine-AuNPs.	38
8: Tauc Plot of uncapped GYY4137-AuNPs with their band gap (E_g).	40
9: Tauc Plot of serine-AuNPs with their band gap (E_g).	40
10: Tauc Plot of serine-AuNPs with their band gap (E_g).	41
11: Colloidal solutions of chitosan capped GYY4137-AuNPs and uncapped GYY4137-AuNPs with precursor solutions**.(a)** GYY4137, (**b)**GYY4137-AuNPs, **(c)**$HAuCl_4^-$,(**d)** chitosan capped GYY4137-AuNPs.	43
12: UV-Vis spectrum of chitosan capped GYY4137-AuNPs.	44
13: Tauc Plot of chitosan capped GYY4137-AuNPs showing band gap (E_g).	44
14: FTIR spectrum of all the reducing agents and gold salt solution prior to synthesis	45
15a: L- serine-AuNPs as per ATR-FTIR image.	46
15b: L- threonine AuNPs as per ATR-FTIR image.	47
15c: Chitosan capped GYY4137 AuNPs as per ATR-FTIR image.	47

UNIVERSITY of the WESTERN CAPE

https://etd.uwc.ac.za

16: Graph of DLS measurements of GYY4137 AuNPs compared to serine -AuNPs and threonine-AuNPs. **a)** GYY4137 AuNPs DLS, **b)** L-threonine AuNPs DLS, and **c)** L-serine AuNPs. 49

17: Graph of surface charge (Z) measurements of GYY4137-AuNPs compared to serine synthesized gold nanoparticles and threonine AuNPs. **a)** GYY4137-AuNPs, **b)** serine-AuNPs and **c)** threonine-AuNPs 50

18: Micrographs of chitosan capped GYY4137-AuNPs and size distribution curve as per HRTEM and STEM. **(a)** Chitosan capped-GYY4137-AuNPs at 0.2µm HRTEM. **(b)**Size distribution of chitosan-capped gold nanoparticles (HRTEM), **c)** chitosan STEM image at 200 nm, **d)** size distribution per STEM image. 52

19: Morphology of serine-AuNPs and distribution curve as per HRTEM image. 52

20: Morphology of threonine-AuNPs as per HRTEM image. 53

21a: Elemental mapping of chitosan capped GYY4137-AuNPs as per EDX image 55

21b: Elemental mapping of L- serine as per EDX image. 55

201c: L- threonine AuNPs as per EDX image. 56

UNIVERSITY of the
WESTERN CAPE

https://etd.uwc.ac.za

List of Tables

Table	Page
1: Examples of commercial nanofertilizers	5
2: Similarities and differences between chitosan and poly ethylene glycol	24
3: Concentration of the gold nanoparticles from Beer's law (A= Ɛbc)	43
4: Spectrum elements and the correlated spectral percentage (%)	54

https://etd.uwc.ac.za

Chapter 1

Chapter Overview

This chapter discusses the advantages of using nanomaterials and nanotechnology as a whole compared to bulk materials. It discusses the use of nanomaterials in agriculture with emphasis on the effects in precision farming and environmental remediation. This includes impact of nano- formulated agrochemicals on plants production, animal in natural habitats, soil quality, microbial diversity and water quality. Furthermore, it discusses the different nanomaterials/particles used to elicit drought tolerance to plants with similar and differing changes caused by these nanomaterials. The main goal of this project is to synthesize and characterize drought enabler GYY4137 (H_2S donor) gold nanoparticles in a nanocomposite and stabilize them with water-soluble polymers poly ethylene glycol and chitosan. The GYY4137 gold nanoparticles were compared to synthesized serine gold nanoparticle and threonine gold nanoparticles. The chapter concludes with the problem statement, aims and objectives of the study.

UNIVERSITY of the
WESTERN CAPE

1. Introduction

1.1. Nanotechnology in biotechnology.

Nanotechnology is science, engineering, and technology conducted at the 10 to 100 one billionth of a metre (Singh *et al*., 2015). Nanotechnology may also can be defined as the technology of manipulating matter to confer materials with unique physical, chemical, magnetic, mechanical and optical properties (Iavicoli *et al*., 2017). Additionally, nanotechnology has benefits such as improvement of food quality and safety, lessening agricultural inputs, enrichment of absorbing nanoscale nutrients from the soil, etc. A number of disciplines such as physics, chemistry, biology and materials science use nanotechnology to progress their applications and use in agriculture (Duhan *et al*., 2017).

Nanoscale materials have quantum effects that are dependent on size, density, electric conductivity and chemical reactivity (Prasad, Bhattacharyya and Nguyen, 2017). Nanomaterials also have large surface to volume ratio which is directly proportional to their high surface energy (Singh *et al*., 2015; Saxena, Tomar and Kumar, 2016).

https://etd.uwc.ac.za

Nanotechnology has enabled electrons to cross barriers to deliver or monitor in vitro in biological systems by a process called tunnelling (Prasad, Bhattacharyya and Nguyen, 2017). The nanomaterials large surface area and high reactivity makes them good catalysts and with fast response delivered in biological systems and safe for short-term use (Prasad, Bhattacharyya and Nguyen, 2017). The nanoparticles are cheaper to synthesize and their level of phytotoxicity is low and depends on the concentration of the nanoparticles (Saxena, Tomar and Kumar, 2016).

Nanoparticles are used in agriculture to use to deliver agrochemicals in a controllable way at selected sites, at an accurate time and in lower quantities (Pérez-de-luque, 2017). Nanoparticles also make selective transportation of genetic material, monitoring, diagnosis and detection of plant and animal diseases and environmental remediation in agriculture possible (Singh *et al*., 2015; Pérez-de-luque, 2017). Nanoparticles are also good candidates for advanced plant breeding programmes and detection or prevention environmental stresses before they affect the food production (Ram, Vivek and Prasad, 2014; Saxena, Tomar and Kumar, 2016).

The number of studies dealing with the interaction between nanomaterials and plants has augmented. Firstly, agriculture deals with more than 7,000 cultivated plant species (Khoshbakht and Hammer, 2008 cited by Pérez-de-Luque, 2017). The plant physiology affects the interaction with nanoparticles what is observed in a crop is not necessarily valid for another one (Pérez-de-Luque, 2017). Nanotoxicity and safety for the environment and human/animal consumption remains to be elucidated (Iavicoli *et al.,* 2017). Finally, consumers do not trust nanotechnology (Duhan *et al*., 2017). In conclusion, nanotechnology has a good potential for applications in agriculture, but there is still a long way down to reach the field (Pérez-de-luque, 2017).The community or the buyer is still not well informed of the use of the nanomaterials on the commercial products (Duhan *et al*., 2017).

UNIVERSITY of the
WESTERN CAPE

1.2. General use of nanomaterials in agriculture.

More than 60 % of the population in developing countries are dependent on agriculture (Ram, Vivek and Kumar, 2014; Singh *et al*., 2015). Agriculture is continuously affected by a growing world population and unfavourable climate conditions (Singh *et al*., 2015; Saxena, Tomar and Kumar, 2016; Iavicoli *et al*., 2017). The food requirement has to increase to meet the population demand (Singh *et al.*, 2015; Saxena, Tomar and Kumar, 2016). Thus, it is vital that plant nutritional scientists focus on precision delivery of

https://etd.uwc.ac.za

nutrients and improve nutrient uptake (Raliya *et al*.,2016; Duhan *et al*., 2017). Nanotechnology is important in sensors, biomarkers, agriculture and environmental enrichment to promote great crop production (Prasad, Bhattacharyya and Nguyen, 2017; Verma *et al*., 2018).

Encapsulation coats chemicals or genetic material to achieve controllable dosage or release and adsorption into plants (Ram,Vivek and Kumar, 2014). Nanocomposites release substances through diffusion, dissolution, biodegradation when they encounter a different environment of pH (Ding and Shah, 2009 cited by Ram, Vivek and Prasad, 2014; Bharadwaj and Singh, 2018). In other industries nanotechnology is well developed compared to its use in the agricultural sector (Duhan *et al.*, 2017).

Most of the studies on nanotechnology are focused on nanoparticles uptake, bio-distribution and toxicity to plants and animals (Duhan *et al*., 2017; Iavicoli *et al.*, 2017; Saxena, Tomar and Kumar, 2016) and on specific target delivery of chemicals, proteins and nucleotides to genetically transform crop (Wang *et al.*, 2014). The marginal application of nanotechnology to agriculture is due to unknown long term impacts of the nanomaterials to humans or the environment (Ram, Vivek and Kumar, 2014; Servin *et al.*, 2015; Verma e*t al.*, 2018).

UNIVERSITY of the
WESTERN CAPE

Nanomaterials mainly help formulate nano-herbicides, nano-pesticide, nano-fertilizers, insecticides, and biosensors to achieve targeted release without harming plants, monitor plants developments or stress or the nearby environment and develop plant growth promoters(Iavicoli *et al*., 2017; de Oliveira *et al.*,2014; Servin *et al*., 2015; Singh *et al*., 2015).Nano-pesticides reduce pathogen and pest resistance, protect soil biodiversity, conserve useful soil microbes; lessen dangers to pollinators and to natural habitats of insects(de Oliveira *et al*., 2014; Mushtaq *et al*.,2018).

Nanomaterials can also be used to determine induction of gene expression related to antioxidant defence machinery to prevent oxidative damage and to simultaneously increase resistance against nanomaterial toxicities (Prasad, Bhattacharyya and Nguyen, 2017; Mushtaq *et al.*, 2018; Verma *et al.*, 2018).

1.2.1. Nanomaterials as fertilizers.

Fertilizers are agrochemicals composed of known quantities of nutrients such as nitrogen, phosphorus and potassium that are vital for plant growth and development(Saxena, Tomar

https://etd.uwc.ac.za

and Kumar, 2016).According to Ram, Vivek and Kumar, (2014) fertilisers plays about 35 to 40 percent in agricultural crop production. Fertilizers provide crop's nutrients and encourage growth and development; however, to improve nutrients use proficiency and change the continuing problem of eutrophication, nanofertilizers are the best alternative. Nanofertilizers have been synthesised for slow controllable dosage of nutrients to plants, to prevent leaching and gasification of nutrients and prevent eutrophication in aquatic environments nearby agricultural lands(Singh *et al.*, 2015; Iavicoli *et al.*, 2017; Prasad, Bhattacharyya and Nguyen, 2017).

Singh *et al.*, (2015) wrote a review on pure metal and metal oxide nanoparticles used as nanofertilizers. Nanoparticles effects on plants is dependent on concentration, size, shape of nanoparticles, surface charge of nanoparticles, type of plant, prior external environmental exposure and defence mechanism of plant (Raliya *et al.*,2016; Pérez-de-luque, 2017). Mostly size is the vital for nanoparticles uptake and transportation into plants (Pérez-de-luque, 2017). The work of Sabo-Attwood *et al*., 2011 and Taylor *et al.*, 2014 reported size limit between 40 and 50 nm of nanoparticles to enable uptake into plant, biodistribution and bioavailability inside the plant cells.

Nanofertilizers enhance plant resistance to salinity stress and drought stress (Mushtaq *et al.*, 2018), elevating the antioxidant enzymes activity and achieving great crop biomass and higher yields (Morales-Diaz *et al.*, 2017). Zinc is an important micronutrient for plant growth and development (Saxena, Tomar and Kumar, 2016). Treatment with 1.2 and 6.8 nm fumigatus zinc oxide nanoparticles of cluster beans, increased their shoot and root length by 22.7% and 43.4% respectively (Raliya and Tarafda, 2013 cited by Servin *et al.*, 2015). The nanoparticles increased total protein (17.2%), chlorophyll (54.5%), and rhizosphere microbial population (13.6%) in comparison to their bulk zinc oxide-treated plants (Raliya and Tarafda, 2013, cited by Servin *et al.*, 2015).

Nanofertilizers can also enhance plants germination rates, photosynthesis; improve the soil quality, microbial biodiversity, compared to conventional fertilizers (Morales-Díaz *et al.*, 2017; Mushtaq *et al.*, 2018). Below are some of the examples of commercial nano-fertilisers available on the market in **Table 1:** Commercial fertilizers made from nano-formulations adapted from: Ram, Vivek and Kumar, 2014).

https://etd.uwc.ac.za

Table 1: Examples of commercial nanofertilizers.

Commercial Product	Content
TAG-Nano (NPK, PhoS, Zinc, Cal etc.) fertilizers	Proteino-lacto-gluconate chelated with micronutrients, vitamins, probiotics, seaweeds extracts and humic acid.
Nano-Gro™	Plant growth regulator and immunity enhancer.
Nano-Green	Extracts of corn, grain, soybeans, potatoes, coconut and palm
Nano-Ag Answer@	Microorganism, sea kelp, and mineral electrolyte.
Biozar Nano-Fertilizer	Combination of organic materials, micronutrients and macromolecules.
Master Nano Chitosan Organic Fertilizer	Water Soluble liquid chitosan, organic acid and salicylic acids, and phenolic compounds.

UNIVERSITY of the
WESTERN CAPE

Commercial fertilizers made from nano-formulations adapted from Prasad, Bhattacharyya, and Nguyen, 2017.

1.2.2. Nanomaterials as Biosensors.

Precision farming uses computers, sensors, and global satellite positioning systems to quantity environmental conditions and assist in influencing whether crops are developing efficiently, detecting the nature and site of complication (Duhan *et al*., 2017). Ultimately, nanotechnology enables agriculturist to monitor, detect and remedy environmental or residual pollutants in real time (Ram, Vivek and Kumar, 2014; Saxena, Tomar and Kumar, 2016). Nano sensors generally monitor crop production and soil quality properties such as water, pH, nutrient levels, temperature and fertility this simplifies application of nutrients, agrochemicals and water only when required (Duhan *et al.*,2017; Iavicoli *et al.*,2017; González-Melendi *et al.*, 2008; Larue *et al.*,2012; Zhao *et al.*, 2012; Sun *et al.*, 2014 cited

https://etd.uwc.ac.za

by Pérez-de-luque, 2017).

Nano sensors are highly sensitive, very selective, have rapid detection time, are portable and have low detection limits (Ram, Vivek and Prasad, 2014; Pérez-de-luque, 2017). The nanoparticles show an electrical or chemical signal in the presence of contaminant on plants (Ram, Vivek and Prasad, 2014; Duhan *et al.,* 2017). Studies have shown that nanoparticles move though the roots and to the leaves via the apoplastic pathway (Sabo-Attwood *et al.*, 2011; Zhai *et al.*, 2014; Wang *et al.*, 2016; Perez du Luque, 2017).

Koo *et al.*, (2015) using gold nanoparticles as sensors showed the nanoparticles root uptake and translocation using their tuneable optical properties resulting in increased temperature across the leaf surface when ablated with laser beam. Koo *et al.*, (2015) proved that the gold nanoparticles were taken up by roots system and moved to the leaves where they induced the expression of heat-shock regulated genes in Arabidopsis thaliana *(et al.,* 2015). On another study Taylor *et al.,* (2014) used 100 mg /l of gold nanoparticles were studied the physiological and genetic responses of *A. thaliana* to presence of the gold nanoparticles. Gold shortened the root length of the seedlings by 75% with oxidized gold (Au^{3+}) in roots and shoots of the plants and reduced gold (Au^{0}) nanoparticles in the root tissues (Taylor *et al.*, 2014). Taylor and co-workers concluded that plants absorb gold in an ionic form and the plants' response to gold presence up-regulate plant defence genes and down-regulate metal transporters to reduce gold nanoparticle uptake (Taylor *et al.*, 2014).

UNIVERSITY of the
WESTERN CAPE

The extent of uptake and biodistribution to plant tissues is dependent on the concentration and also the type of gold nanoparticles (Sabo-Attwood *et al.*, 2011). Yin *et al.*, (2015) reported that a 10 µg/mL concentration of sodium upconversion nanoparticles promoted roots and stems growth in Glycine max. However, at higher than 50 µg/mL concentration the hindered the growth and that the nanoparticle entered as cluster-like Y-phosphate through the roots and then moved through vessels to stems and leaves (Yin *et al.*, 2015).

Fluorescently labelled maghemite nanoparticles (20 mg. L^{-1}) monitored the iron uptake in watermelon plants (Wang *et al.*, 2016). The TEM micrographs showed that the nanoparticles penetrated the root, moved from the epidermis to endodermis through the apoplastic pathway (Wang *et al.*, 2016). The γ-Fe_2O_3 NPs (20 mg/L) had no oxidative stress on watermelon, however, at 50 mg. L^{-1} γ-Fe_2O_3 NPs could increase soluble sugar, soluble protein and chlorophyll content in the growth of plants (Wang *et al.*, 2016).

https://etd.uwc.ac.za

Quantum dots can be used as a sensor and are suitable for bio-marking the whole cell (Koo *et al.*, 2015). The fluorescence property of cadmium selenide/cadmium zinc selenide quantum dots were used for bio-marking the structure of *Arabidopsis thaliana* (Koo *et al.*, 2015). The study showed that the quantum dots were absorbed through leaf petioles and roots and uniformLy distributed in leaves (Koo *et al.*,2015).

1.2.3. The nanomaterials as plant protecting products.

Plant protecting products include pesticide, herbicide, insecticide and fungicides (Kim *et al.*, 2012; Van Nhan *et al.*,2015; Le Van *et al.*, 2016). The use of nano-formulations protects the environment due to faster disappearance of the gas released by the chemicals used to protect the plants (Pérez-de-luque, 2017). Nano-encapsulations targeted release of chemicals reduces the risk of species resistance against the chemicals (Ram, Vivek and Kumar, 2014). The nano-formulations prevent high rate of application of plant protecting products and prevent bio-magnification (Ram, Vivek and Prasad,2014; Duhan *et al.*, 2017; Pérez-de-luque, 2017).

A 10 mg/l of copper oxide nanoparticles applied in transgenic and conventional cotton to check their effect on Bacillus thuringiensis (Bt) toxin Bt gene (Le Van *et al.*, 2016). The copper oxide nanoparticles enhanced the expression of the exogenous Bt gene encoding protein in transgenic leaves and roots. The application promoted the Bt cotton's insect resistance in the plants (Le Van *et al.*, 2016). The Bt toxin is the product of an exogenous Bt gene, whose concentration in shoots is the most important index for evaluating the insect resistant ability of Bt cotton (Van Nhan *et al.*, 2015).

The application of 100 $mg \cdot L^{-1}$iron oxide nanoparticles increased the Bt toxin concentrations in leaves and roots to 845.89 and 886.94 $ng \cdot g^{-1}$, respectively, more than 1.61 and 1.36 times than conventional cotton control group. However, at 1000 $mg \cdot L^{-1}$ the Bt toxin decrease in B t cotton plant although were still greater ($p < 0.05$) than that of the control group. The elevation of Bt toxin in leaves at 100 mg·L-1 could be vital for resisting insect damage and serve as a prerequisite for variations in the efficiency of Bt genes and the application of nanoparticles in agriculture (Van Nhan *et al.*, 2015).

Silver nanoparticles have been used as fungicide, pesticide and herbicide to protect plants due to their antimicrobial ability(Saxena, Tomar and Kumar, 2016). 200mg/l of silver nanoparticles were used as a fungicide and reduce phytopathogenic fungi *Bipolaris*

https://etd.uwc.ac.za

sokoniana (*Sacc*)and *Magnoporthe grisea* colonies (Jo *et al.*, 2009). As the concentration of silver nanoparticles increased it reduced the conidia of both fungi by 50% in perennial ryegrass compared to silver ions (Jo *et al.*, 2009).

Nanomaterials can be used for genetic material delivery into a specific host organelle for protection without causing phytotoxicity (Torney *et al.*, 2007). Torney *et al.*, (2007) reported the efficient delivery of deoxyribonucleic acid (DNA) and chemicals using silica nanoparticles internalized in plant cells for growth and development of plants. Herewith at the bottom, **Fig.1** shows the utility of nanomaterial in agriculture (Adapted from Iavicoli *et al.*, 2017).

UNIVERSITY of the
WESTERN CAPE

https://etd.uwc.ac.za

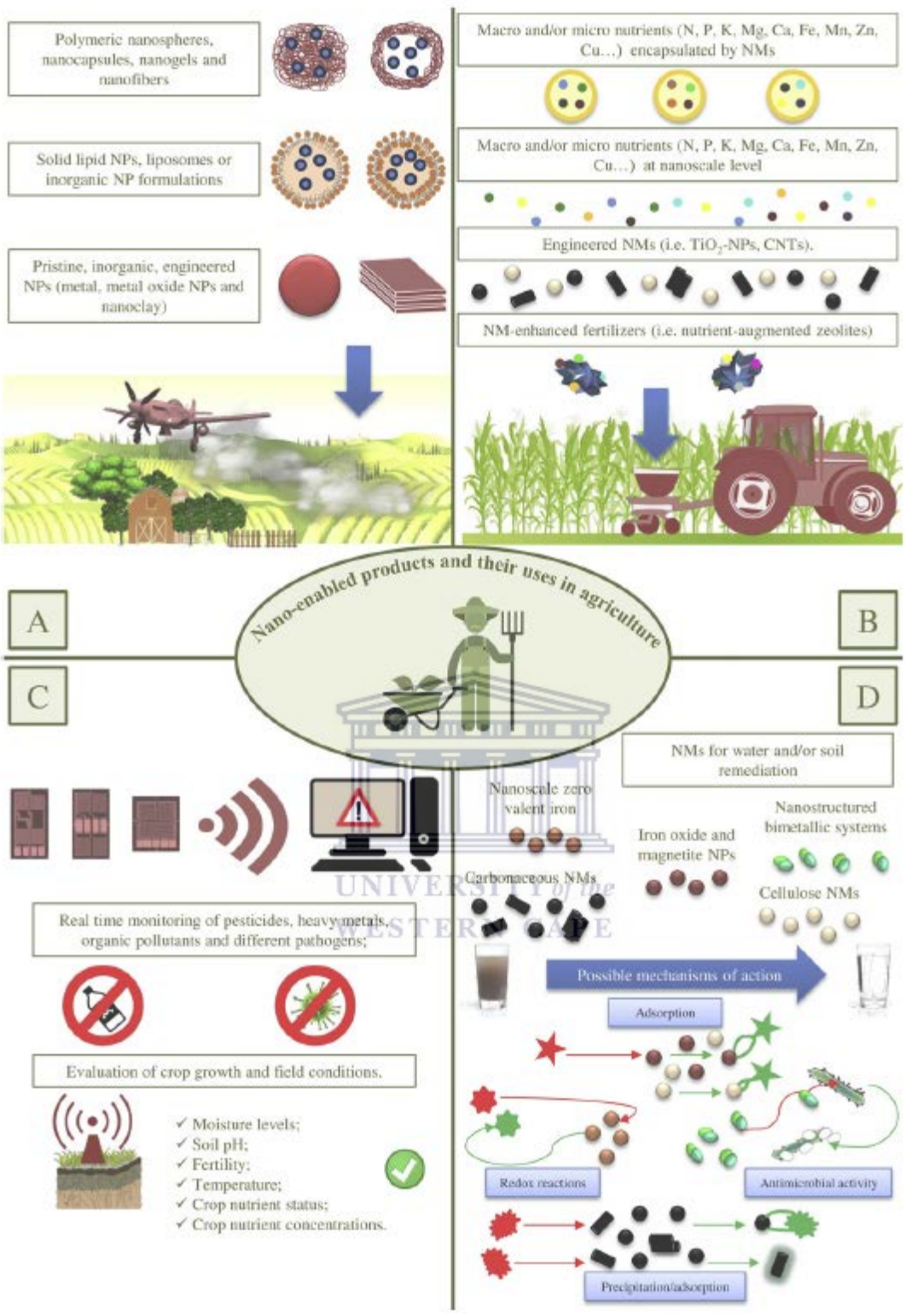

Figure 1: The applications of nanomaterial in agriculture. **A)** Nano-pesticide formulations; **B)** Nano-fertilisers; **C)** Biosensors and **(D)** Nano-products for water and soil remediation. (Adapted from Iavicoli *et al.*, 2017).

https://etd.uwc.ac.za

1.3. Nanomaterials improve drought tolerance.

Drought is a major abiotic stress disturbing crop growth and yield worldwide due to oxidative stress that reduce plant photosynthesis (Djanaguiraman *et al.,* 2018). Drought elevates reactive species, cause high production of secondary metabolites to adjust the membrane fluidity and antioxidants to defend plants against the environmental stimuli (Siddiqi and Husen, 2016). Morales-Diaz and co-workers, (2017), stated that keeping mineral nutrients balanced, metabolites, signal molecules and antioxidants or osmolytes at thresholds provides a good chance of plants acclimatizing to the environment and that there may be a relationship between nutritional quality of crops and the stress tolerance of plants.

Nanoparticles have been shown to elicit modifications in plants in a concentration, species specific and exposure dependent manner (Saxena, Tomar and Kumar, 2016; Duhan *et al.*, 2017). Researchers are continuously investigating nanoparticles for alleviation of drought stress as a way to mitigate and increase agricultural reproduction using pure metals, metal oxides and carbonaceous nanomaterials among them (Saxena, Tomar and Kumar, 2016).

1.3.1. Inorganic nanomaterials improve plants drought tolerance.

Most metal oxide nanoparticles have the ability of influencing the growth and development of plants (Ram, Vivek and Prasad, 2014; Verma *et al.*, 2018). The zinc and copper micronutrients are vital micronutrients needed for the optimum growth and development of plants (Saxena, Tomar and Kumar, 2016). Pre-treatment with part of mother colloid solution to 100 parts of water of two winter wheat seeds variety with zinc oxide and copper oxide colloidal nanoparticles have shown a species-specific reduction of drought stress (Taran *et al.*, 2017). The *steppe Acveduc* (by 30%) variety was more drought tolerant than *Stolichna* (by 27%) by evidence of elevation of antioxidant enzymes superoxide dismutase (SOD) and catalase (CAT), lower reactive species and lipid peroxidation. Furthermore, the colloidal solution presented stable wheat photosynthetic pigments and high relative water content in the wheat leaves (Taran *et al.*, 2017).

Exogenous application of 30, 50 and 100 ppm to Moldavian balm herbaceous plant was effective for increasing phenolic compounds (Faghih *et al.*, 2017, 2019 cited by Kamalizadeh, Bihamta and Zarei, 2019). Plants generally increase different phenolic compounds, improve plant antioxidant systems and improve tolerance to the stress (Faghih *et al.*, 2017, 2019 cited by Kamalizadeh, Bihamta and Zarei, 2019). The combination of

https://etd.uwc.ac.za

drought stress and anatase nanoparticles had no significant effect on most phenolic compounds, except on chlorogenic acid, which increased significantly by application of titanium nanoparticles.

Wheat application to silicon (Si) nanoparticles (0, 30, 60 ppm) increased the leaf greenness, crop yield, proline, superoxide enzyme activity and water content in plants under both soil and foliar spraying application regimes in wheat plants during drought stress (Behboudi *et al.*, 2018). Magnetite nanoparticles and maghemite nanoparticles have provided good basis of nanofertilizers to improve drought stress in canola plants (Palmqvist *et al.*, 2017). Particularly, maghemite resulted in reduced hydrogen peroxide levels, and lipid peroxidation, enhanced leaves growth rate and chlorophyll content compared to control plants suggesting that maghemite nanoparticles provided drought tolerance to the plants in drought stress conditions and good alternative to supplement of nutrient chelated ion.

The application of nanoceria (10 mg.L^{-1}) effectively reduced leaf reactive oxygen species ,germination and seed yield per plant by 41%, 31%, and 31%respectively in drought-stressed plants comparative to control sorghum plants through a root to shoot translocation route (Djanaguiraman *et al.*, 2018).

1.3.2. Carbonaceous nanomaterials in drought tolerance.

Borišev *et al.*, (2016) reported that 70µmol/l and 700µmol/l fullerenol nanoparticles protected sugar beet from both moderate and severe drought stress. Fullerenol bound large amounts of water acting as a compatible osmolyte to serve as an additional intracellular supply of water for the plants (Borišev *et al.*,2016). The soil relative water content between 60-70% reduced roots proline and elevated antioxidant enzyme activities in a fullerenol concentration dependent manner (Borišev *et al.*, 2016).

Wang *et al.*, (2014) examined 20% (PEG 6000) drought stress with 10–1000 mg. L^{-1} graphene oxide nanoparticles in Arabidopsis thaliana seedlings effect on drought stress expression genes. The combination of PEG 6000 with 1000 mg L^{-1} of the nanoparticles significantly decreased the expression level of HKT1 and elevated in the expression levels of ABI4, ABI5, AREB1, SOS1, and RD29A compared to PEG 6000 (20%) treated plant (Wang *et al.*, 2014). The genes ABI4, ABI5, AREB1, HKT1, SOS1, and RD29A are required for the control of drought and/or salt stress, thus carbon nanomaterials may have the ability to provide stress tolerance in plants (Wang *et al.*, 2014).

https://etd.uwc.ac.za

1.4. The GYY4137 effect on drought stress.

It is well known that plants protect themselves against environmental factors such as drought by producing a lot of signalling molecules including hydrogen sulfide (H_2S) among others (Garcia –Mata and Lamattina, 2012). The signalling molecule is involved in seed germination, plant growth and development and in drought stress tolerance (Li, Min and Zhou, 2016). Garcia-Mata and Lamattina (2010) has shown that one to 500 µM GYY4137 induced stomatal closure in *Vicia faba*, *Arabidopsis thaliana* and *Impatiens wallerians* during drought in a dose dependent manner. The regulation of the stomatal apertures happened through a modification of the guard cells and osmotic rearrangements in plants. This resulted in regulation of carbon dioxide used by plants, photosynthesis and limited water loss as water vapour (Garcia-Mata and Lamattina, 2010). The H_2S stomatal closure was concluded to have happened through ABC transporters regulation using an abscisic acid -dependent pathway (Garcia-Mata and Lamattina, 2010).

Previously used H_2S donors have been used to protect crops against drought stress, but they released H_2S in a short burst and not mimicking a biological sample (Christou *et al.*, 2013; Shen *et al.*, 2013; Kang, Neil and Xian, 2017). Honda *et al.*, (2015) showed that using 100 mM GYY4137 induced stomatal closure for the first 90 minutes and thereafter 120 min with 100 mM GYY4137 the stomata fully reopened. Some work done on GYY4137 has shown that H_2S that work in concert with nitric oxide (Honda *et al.*, 2015) and abscisic acid (Garcia-Mata and Lamattina, 2010) to promote growth of plants. However, the exact mechanism of H_2S signalling remains to be elucidated (Garcia-Mata and Lamattina 2010: Garcia-Mata and Lamattina, 2012). The H_2S accumulation from 500µM sodium hydrosulfide (NaHS) treatment was rapid than that of GYY4137 and at high concentrations the gas causes phytotoxicity (Garcia-Mata and Lamattina, 2012).

UNIVERSITY of the
WESTERN CAPE

1.5. Comparison of GYY4137 to NaHS.

Morpholin-4-ium 4-methoxyphenyl (morpholino) phosphinodithioate (GYY4137) is a H_2S donor that releases the gas slowly over extended period of time (Li *et al.*, 2008; Carter *et al.*, 2018). GYY4137 is pH and temperature dependent (Li *et al.*, 2008). Its ability to release H_2S at slower rate makes it a donor choice for working on biological samples (Rose, Dymock, and Moore, 2015). GYY4137 also shares some useful properties with other donors such sodium hydroxide (NaHS) such as of the anticancer abilities, anti-inflammation, good water-solubility, and ability to make plants stress tolerant (Rose,

https://etd.uwc.ac.za

Dymock, and Moore, 2015; Garcia –Mata and Lamattina, 2012). Although the NaHS has prompted research on H_2S it generates undesirable large amounts of H_2S in short time and is easy to obtain and it is widely used in the preparation of H_2S solutions (Kang, Neil and Xian, 2017).

1.6. Problem Statement

Climate conditions have caused worldwide drought, exacerbated malnutrition and famine in lot of Sub-Saharan African countries. Several H_2S donors have been used to alleviate drought and other biotic stresses. Nevertheless, they release too much of the gas one time, hence GYY4137 has been reported to alleviate drought stress and can release H_2S slowly as for long period as in biological samples. However, GYY4137 has not been utilised at nano-level. Therefore, there is a need to make nano agrochemicals that will enhance drought tolerance such as GYY4137 (H_2S donor) for application to drought stress relief in plants.

1.7. Research aims and objectives

The aim of this project was to synthesize GYY4137 gold nanoparticles (GYY4137-AuNPs), stabilize with them water soluble polymers poly ethylene glycol (PEG) and chitosan and characterize the polymer GYY4137 gold nanoparticles.

Objectives:

- Synthesize GYY4137 –capped gold nanoparticles using reflux reduction synthesis procedure.
- Synthesize serine gold nanoparticles and threonine AuNPs for comparison with GYY4137 AuNPs.
- Stabilize the nanoparticles using water soluble polymers; poly (ethylene) glycol (PEG) and chitosan.
- Characterize the GYY4137-AuNPs using the standard microscopic and spectroscopic characterization techniques compared to both serine-AuNPs and threonine-AuNPs.

UNIVERSITY of the
WESTERN CAPE

https://etd.uwc.ac.za

1.8. References

1. Bharadwaj, D., and Singh, S. (2018). Nanobiotechnology in Agriculture. In D. N. Bharadwaj (Ed.) Advanced Molecular Plant Breeding: Meeting the Challenge of Food Security (pp. page range of chapter). New York: Apple Academic Press:https://doi.org/10.1201/b22473
2. Behboudi, F., Tahmasebi Sarvestani, Z., Kassaee, M., . Modares Sanavi, S., Sorooshzadeh, A. (2018).Improving Growth and Yield of Wheat under Drought Stress via Application of SiO_2 Nanoparticles, *Jounal of Agricultural Science and Technology*, 20 (7), pp. 1479–1492.
3. Borišev, M., Borišev, I., Župunski, M., Arsenov, D., Pajević, S., Ćurčić, Ž., Vasin, J. and Djordjevic, A. (2016). Foliar Application of Fullerenol Nanoparticles alleviates drought Impact in Sugar Beets (*Beta vulgaris L.*) *PLOS ONE*, 11(11), p. e0166248.
4. Carter, J., Brown, E., Grace, J., Salem, A., Irish, E. and Bowden, N. (2018). Improved growth of pea, lettuce, and radish plants using the slow release of hydrogen sulfide from GYY-4137. *PLOS ONE*, 13(12), p. e0208732.
5. Christou, A., Manganaris, G., Papadopoulos, I. and Fotopoulos, V. (2013). Hydrogen sulfide induces systemic tolerance to salinity and non-ionic osmotic stress in strawberry plants through modification of reactive species biosynthesis and transcriptional regulation of multiple defence pathways. *Journal of Experimental Botany*, 64(7), pp.1953-1966.
6. Djanaguiraman, M., Nair, R., Giraldo, J. and Prasad, P. (2018). Cerium Oxide Nanoparticles Decrease Drought-Induced Oxidative Damage in Sorghum Leading to Higher Photosynthesis and Grain Yield. *ACS Omega*, 3(10), pp.14406-14416.
7. Duhan, J., Kumar, R., Kumar, N., Kaur, P., Nehra, K. and Duhan, S. (2017). Nanotechnology: The new perspective in precision agriculture. *Biotechnology Reports*, 15, pp.11-23.
8. García-Mata, C. and Lamattina, L. (2010). Hydrogen sulphide, a novel gasotransmitter involved in guard cell signalling. *New Phytologist*, 188(4), pp.977-984.
9. García-Mata, C. and Lamattina, L. (2012). Gasotransmitters are emerging as new guard cell signalling molecules and regulators of leaf gas exchange. *Plant Science*, 201-202, pp.66-73.

UNIVERSITY of the WESTERN CAPE

https://etd.uwc.ac.za

10. Honda, K., Yamada, N., Yoshida, R., Ihara, H., Sawa, T., Akaike, T. and Iwai, S. (2015). 8-Mercapto-Cyclic GMP Mediates Hydrogen Sulfide-Induced Stomatal Closure in *Arabidopsis*. *Plant and Cell Physiology*, 56(8), pp.1481-1489.
11. Iavicoli, I., Leso, V., Beezhold, D. and Shvedova, A. (2017). Nanotechnology in agriculture: Opportunities, toxicological implications, and occupational risks. *Toxicology and Applied Pharmacology*, 329, pp.96-111.
12. Jain, P., Lee, K., El-Sayed, I. and El-Sayed, M. (2006). Calculated Absorption and Scattering Properties of Gold Nanoparticles of Different Size, Shape, and Composition: Applications in Biological Imaging and Biomedicine. The Journal of Physical Chemistry B, 110(14), pp.7238-7248
13. Jo, Y., Kim, B. and Jung, G. (2009). Antifungal Activity of Silver Ions and Nanoparticles on Phytopathogenic Fungi. *Plant Disease*, 93(10), pp.1037-1043.
14. Judy, J. D., Unrine, J. M., Rao, W., Wirick, S., and Bertsch, P. M. (2012). Bioavailability of gold nanomaterials to plants: importance of particle size and surface coating. *Environmental Science and Technology*. 46, 8467–8474.
15. Kamalizadeh, M., Bihamta, M. and Zarei, A. (2019). Drought stress and TiO_2 nanoparticles affect the composition of different active compounds in the Moldavian dragonhead plant. *Acta Physiologiae Plantarum*, 41(21).
16. Kim, S., Jung, J., Lamsal, K., Kim, Y., Min, J. and Lee, Y. (2012). Antifungal Effects of Silver Nanoparticles (AgNPs) against Various Plant Pathogenic Fungi. *Mycobiology*, 40(1), pp.53-58.
17. Koelmel, J., Leland, T., Wang, H., Amarasiriwardena, D. and Xing, B. (2013). Investigation of gold nanoparticles uptake and their tissue level distribution in rice plants by laser ablation-inductively coupled-mass spectrometry. *Environmental Pollution*, 174, pp.222-228.
18. Koo, Y., Wang, J., Zhang, Q., Zhu, H., Chehab, E., Colvin, V., Alvarez, P. and Braam, J. (2014). Fluorescence Reports Intact Quantum Dot Uptake into Roots and Translocation to Leaves of *Arabidopsis thaliana* and Subsequent Ingestion by Insect Herbivores. *Environmental Science & Technology*, 49(1), pp.626-632.
19. Koo, Y., Lukianova-Hleb, E., Pan, J., Thompson, S., Lapotko, D. and Braam, J. (2015). In Planta Response of *Arabidopsis* to Photothermal Impact Mediated by Gold Nanoparticles. Small, 12(5), pp.623-630.

UNIVERSITY of the
WESTERN CAPE

https://etd.uwc.ac.za

20. Le Van, N., Ma, C., Shang, J., Rui, Y., Liu, S. and Xing, B. (2016). Effects of CuO nanoparticles on insecticidal activity and phytotoxicity in conventional and transgenic cotton. *Chemosphere*, 144, pp.661-670.
21. Li, L., Whiteman, M., Guan, Y., Neo, K., Cheng, Y., Lee, S., Zhao, Y., Baskar, R., Tan, C. and Moore, P. (2008). Characterization of a Novel, Water-Soluble Hydrogen Sulfide–Releasing Molecule (GYY4137). *Circulation*, 117(18), pp.2351-2360.
22. Li, Z., Min, X. and Zhou, Z. (2016). Hydrogen Sulfide: A Signal Molecule in Plant Cross-Adaptation. *Frontiers in Plant Science*, 7, 1621.
23. Morales-Díaz, A., Ortega-Ortíz, H., Juárez-Maldonado, A., Cadenas-Pliego, G., González-Morales, S. and Benavides-Mendoza, A. (2017). Application of nanoelements in plant nutrition and its impact in ecosystems. Advances in Natural Sciences: *Nanoscience and Nanotechnology*, 8(1), p.013001.
24. Mushtaq, A., Jamil, N., Rizwan, S., Mandokhel, F., Riaz, M., Hornyak, G., Najam, Malghani, M. and NaeemShahwani, M. (2018). Engineered Silica Nanoparticles and silica nanoparticles containing Controlled Release Fertilizer for drought and saline areas. *IOP Conference Series: Materials Science and Engineering*, 414, p.012029.
25. Navarro, D., Bisson, M. and Aga, D. (2012). Investigating uptake of water-dispersible CdSe/ZnS quantum dot nanoparticles by *Arabidopsis thaliana* plants. *Journal of Hazardous Materials*, 211-212, pp.427-435.
26. De Oliveira, J., Campos, E., Bakshi, M., Abhilash, P. and Fraceto, L. (2014). Application of nanotechnology for the encapsulation of botanical insecticides for sustainable agriculture: Prospects and promises. *Biotechnology Advances*, 32(8), pp.1550-1561.
27. Palmqvist, N., Seisenbaeva, G., Svedlindh, P. and Kessler, V. (2017). Maghemite Nanoparticles Acts as Nanozymes, Improving Growth and Abiotic Stress Tolerance in Brassica napus. *Nanoscale Research Letters*, 12(1).
28. Pérez-de-Luque, A. (2017). Interaction of Nanomaterials with Plants: What Do We Need for Real Applications in Agriculture? *Frontiers in Environmental Science*, 5.
29. Prasad, R., Bhattacharyya, A. and Nguyen, Q. (2017). Nanotechnology in Sustainable Agriculture: Recent Developments, Challenges, and Perspectives. *Frontiers in Microbiology*, 8.
30. Raliya, R., Franke, C., Chavalmane, S., Nair, R., Reed, N. and Biswas, P. (2016). Quantitative Understanding of Nanoparticle Uptake in Watermelon Plants. *Frontiers in Plant Science*, 7.

UNIVERSITY of the WESTERN CAPE
https://etd.uwc.ac.za

31. Ram, P., Vivek, K. and Kumar, S. (2014). Nanotechnology in sustainable agriculture: Present concerns and future aspects. *African Journal of Biotechnology*, 13(6), pp.705-713.
32. Sabo-Attwood, T., Unrine, J., Stone, J., Murphy, C., Ghoshroy, S., Blom, D., Bertsch, P. and Newman, L. (2011). Uptake, distribution and toxicity of gold nanoparticles in tobacco (*Nicotianaxanthi*) seedlings. *Nanotoxicology*, 6(4), pp.353-360.
33. Saha, K., Agasti, S., Kim, C., Li, X. and Rotello, V. (2012). Gold Nanoparticles in Chemical and Biological Sensing. *Chemical Reviews*, 112(5), pp.2739-2779.
34. Saxena, R., Tomar, R. and Kumar, M. (2016). Exploring Nanobiotechnology to Mitigate Abiotic Stress in Crop Plants. *Journal of Pharmaceutical Sciences and Research*, 8(9), pp. 974–980.
35. Servin, A., Elmer, W., Mukherjee, A., De la Torre-Roche, R., Hamdi, H., White, J., Bindraban, P. and Dimkpa, C. (2015). A review of the use of engineered nanomaterials to suppress plant disease and enhance crop yield. *Journal of Nanoparticle Research*, 17(2).
36. Shen, J., Xing, T., Yuan, H., Liu, Z., Jin, Z., Zhang, L. and Pei, Y. (2013). Hydrogen Sulfide Improves Drought Tolerance in *Arabidopsis thaliana* by microRNA Expressions. *PLoS ONE*, 8(10), p. e77047.
37. Singh, A., Singha, A., Hussaina, I., Singha, H and Singh, S. (2015). Plant-nanoparticle interaction : An approach to improve agricultural practices and plant productivity. *International Journal of Pharmaceutical Science Invention*, 4(8), pp. 25–40.
38. Taran, N., Storozhenko, V., Svietlova, N., Batsmanova, L., Shvartau, V. and Kovalenko, M. (2017). Effect of Zinc and Copper Nanoparticles on Drought Resistance of Wheat Seedlings. *Nanoscale Research Letters*, 12(1).
39. Taylor, A., Rylott, E., Anderson, C. and Bruce, N. (2014). Investigating the Toxicity, Uptake, Nanoparticle Formation and Genetic Response of Plants to Gold. *PLoS ONE*, 9(4), p. e93793.
40. Torney, F., Trewyn, B., Lin, V. and Wang, K. (2007). Mesoporous silica nanoparticles deliver DNA and chemicals into plants. *Nature Nanotechnology*, 2(5), pp.295-300.
41. Van Nhan, L., Ma, C., Rui, Y., Cao, W., Deng, Y., Liu, L. and Xing, B. (2016). The Effects of Fe_2O_3 Nanoparticles on Physiology and Insecticide Activity in Non-Transgenic and Bt-Transgenic Cotton. *Frontiers in Plant Science*, 6.

UNIVERSITY of the WESTERN CAPE

https://etd.uwc.ac.za

42. Verma, S., Das, A., Patel, M., Shah, A., Kumar, V. and Gantait, S. (2018). Engineered nanomaterials for plant growth and development: A perspective analysis. *Science of the Total Environment*, 630, pp.1413-1435.
43. Wang, Q., Zhao, S., Zhao, Y., Rui, Q. and Wang, D. (2014). Toxicity and translocation of graphene oxide in *Arabidopsis* plants under stress conditions. *RSC Advances.*, 4(105), pp.60891-60901.
44. Wang, Y., Hu, J., Dai, Z., Li, J. and Huang, J. (2016). In vitro assessment of physiological changes of watermelon (*Citrullus lanatus*) upon iron oxide nanoparticles exposure. *Plant Physiology and Biochemistry*, 108, pp.353-360.
45. Yeh, Y., Creran, B. and Rotello, V. (2012). Gold nanoparticles: preparation, properties, and applications in bionanotechnology. *Nanoscale*, 4(6), pp.1871-1880.
46. Yin, W., Zhou, L., Ma, Y., Tian, G., Zhao, J., Yan, L., Zheng, X., Zhang, P., Yu, J., Gu, Z. and Zhao, Y. (2015). Phytotoxicity, Translocation, and Biotransformation of NaYF4Upconversion Nanoparticles in a Soybean Plant. *Small*, 11(36), pp.4774-4784.
47. Zarabi, M., Arshadi, N., Farhangi, A. and Akbarzadeh, A. (2013). Preparation and Characterization of Gold Nanoparticles with Amino Acids, Examination of Their Stability. *Indian Journal of Clinical Biochemistry*, 29(3), pp.306-314.

UNIVERSITY of the
WESTERN CAPE

https://etd.uwc.ac.za

Chapter 2

Literature review

Chapter Overview

This chapter consists of literature review describing the AuNPs, their general applications and methods used to synthesise them. The review highlights several applications and work done so far on agriculture using AuNPs nanoparticles focusing on reviews of how the properties of the gold nanoparticles make it a nanocomposite of choice when working in agriculture. This is followed by a review of GYY4137 general chemistry or structural and biological properties. Finally, polymers (PEG and chitosan) used are discussed and what they have in common and their differences are presented in a tabular form.

2.1. History of gold nanoparticles.

Gold nanoparticles as metallic nanoparticles are the preferred choice of nanoparticles due to their tuneable optical and physic-chemical properties that allow manipulative control of size, composition, assembly and bio conjugation (Huang *et al.*, 2007; Jain *et al.*, 2006; Kumar *et al.*, 2013). The gold nanoparticles also a have simple and rapid synthetic procedures. The synthesis of gold nanoparticles go as far back to Michael Faraday's work in 1857, in which the gold hydrosols were prepared by reduction of an aqueous solution of gold (iii) chloride with phosphorus dissolved in carbon disulphide (Faraday,1859 cited by Saha *et al.*, 2012) Gold colloids are the most stable and synthesized by either citrate reduction method or by the Brust-Schiffrin method (Daniel and Astruc, 2004).The citrate reduction method uses citrate ions reduce gold(III) chloride in water to synthesise spherical nanoparticles, and was invented by Turkevich in 1951 cited by Daniel and Astruc, 2004).

The size of the nanoparticles can be controlled by changing the concentration of the citrate (Huang *et al.*, 2007). Following that Frens, (1973) optimised the latter method by using different ratios of reducing agents to stabilizing agent and synthesised nanoparticles size between16 nm and 147 nm in solution (Daniel and Astruc,2004; Yeh, Creran, and. Rotello, 2012). Thereafter, the two-phase Brust-Schiffrin method followed in 1994 and synthesised thermally stable and air-stable AuNPs with sizes between 1.5 and 5.2 nm (Daniel and Astruc, 2004). The Brust-Schiffrin method enabled synthesis of highly dispersed

UNIVERSITY of the WESTERN CAPE

https://etd.uwc.ac.za

nanoparticles, with low probability of agglomeration and allowed stabilizing colloids with variety of functional thiol ligands (Daniel and Astruc, 2004). The DNA, peptides and antibodies can also be used to cap the gold nanoparticles by means of covalent and non-covalent interactions (Huang *et al.*, 2007; Saha *et al.*, 2012).

2.2. General properties and applications of gold nanoparticles.

Gold nanoparticles offer electronic and chemical properties, which make them the focus of extensive research (Piella, Bastús and Puntes, 2015; Saha *et al.*, 2012; Zarabi *et al.*, 2013). Gold nanoparticles have strong binding affinity for thiols, disulphide and amines making them good in biological applications (Piella, Bastús and Puntes, 2015). The gold nanoparticles properties are diameter and shape dependent (Daniel and Astruc, 2004). AuNPs are applied in optoelectronic devices, ultrasensitive chemical and biological sensors, and as catalysts in chemical and photochemical reactions (Saha *et al.*, 2012).

Gold nanoparticles are easy and rapid to synthesize and encapsulate with different ligands (DNA, peptides etc.) and highly sensitive and specific for targeted delivery (Jain *et al.*,2006; Saha *et al.*, 2012). Wangoo *et al.*, (2014) reported that gold nanoparticles bio-safety in human cells was established and that they are non-susceptible to photo-bleaching and/ or chemical damage. Colloidal AuNPs aqueous solutions generally show an absorption peak from 500 to 550 nm (Jain *et al.*, 2006; Yeh, Creran, and Rotello, 2012).

UNIVERSITY of the
WESTERN CAPE

Gold nanoparticles have a quantum size effect that leads to discrete electron transition energy levels (Saha *et al.*, 2012). Moreover, the quantization of gold nanoparticles may be changed by external ligands, magnetic fields and electrolyte ions (Saha *et al.*, 2012). The surface absorption peak is due to collective oscillation of the conduction electrons from the resonance excitation by the incident photons, which is termed “surface resonance plasmon peak” (Daniel and Astruc, 2004; Yeh, Creran, and Rotello, 2012). This peak is influenced by size, shape of the nanoparticle, solvent, ligand, core charge, temperature and interparticle distance (Daniel and Astruc, 2004, Judy *et al.*, 2012; Yeh, Creran, and Rotello, 2012: Saha *et al.*,2012). A major problem to some gold nanoparticles is their inability to stay stable long enough for application in biological systems (Saha *et al.*,2012; Que *et al.*,2015). According to Que *et al.*, (2015), the Au-to-thiol bond is a Lewis acid-based interaction and is affected by salt, pH, and external thiol compounds leading dissociation of the Au-to-thiol bond. Thus, its suitability for biomedicine and catalysis is affected because the

https://etd.uwc.ac.za

nanoparticles need to be stable in solutions rich in salt and thiol compounds (Que *et al.*,2015).

2.3. Studies of gold nanoparticles in agriculture

Gold nanoparticles effects on plant physiology, development and metabolism are very limited (Kumar *et al.*, 2013). When dealing with the utility of gold nanoparticles in agriculture most studies have dealt mainly with uptake, translocation, biodistribution, bioavailability, and toxicity and growth improvement in plants (Zhai *et al.*, 2014). The gold nanoparticles are the least examined in relation to germination, water balance, nutrition, genotoxicology or seed production for which the impact of AuNPs is unknown (Milewska-Hendel *et al.*, 2017). Investigation of uptake of gold nanoparticles showed that gold is transported in an ionic (Au^{3+}) water soluble form from the roots to the leaves and then reduced to gold metal nanoparticles (Au^{0}) and accumulated within the woody poplar cells (Zhai *et al.*, 2014).

Taylor *et al.*, (2014) showed a translocation route for gold nanoparticles using 100 mg L^{-1} through the physiological and genetic responses of *A. thaliana* (L.), where the gold shortened the roots length of the seedlings by 75% with oxidized Au^{3+} in roots and shoots of the plants and Au^{0} nanoparticles in the root tissues. Taylor and co-workers concluded that plants absorb gold as an ionic form and the plants' response to presence of gold up-regulate plant defence genes and may down-regulate metal transporters to reduce gold uptake (Taylor *et al.*, 2014), this study was also supported previous studies of Sabo-Attwood *et al.*, 2011 and Koelmel *et al.*, (2013).

Gold nanoparticles uptake and translocation route was also shown in a different plant woody poplar by Zhai *et al.*, 2014 research study using 15 nm, 25 nm and 50 nm AuNPs. The effects of AuNPs dependent on dose or concentration of nanoparticles (and on type of species or size and coating of AuNPs (Shah and Belozerova, 2008; Judy *et al.*, 2012; Kumar *et al.*, 2013; Zhai *et al.*, 2014; Taylor *et al.*, 2014; Siddiqi and Hussen, 2016). The lettuce was treated with 0.013 % (w/w) dodecanethiol-functionalised gold nanoparticles for 15 days (Shah and Belozerova, 2008). The treatment significantly increased the ratio of shoot length to root length by *P* values of 0.008 (Shah and Belozerova, 2008). There is a growth in the shoot/root ratio for the gold nanoparticles treated plants compared to that of the control indicating that these nanoparticles do affect the growth of the plants (Shah and Belozerova, 2008).

https://etd.uwc.ac.za

Treatment of plants with 24 nm of gold nanoparticles containing 10 and 80 µg. $mL^{-1}$was used to determine the nanoparticle's effect on antioxidant enzyme activity and micro RNAs of *A. Thaliana* (Kumar *et al.*, 2013). The 24 nm of gold nanoparticles reduced the reactive oxygen species production by 3.54 and 2.59 folds by elevating scavenging enzymes such as superoxide dismutase (1.83 and 2.83), ascorbate peroxidase (1.24 and 1.78), catalase (1.42and 2.41), and glutathione reductase (1.48 and 2,35).

The miRNA expression pattern miR164, miR167, miR169, miR319, miR395, miR397, miR398, miR399, miR408 and miR414 involved in seed germination and plant physiology were analysed (Kumar *et al.*, 2013). The 80 µg. mL^{-1} significantly downregulated the expression of 6 miRNAs compared to control seedlings and 10 µg. mL^{-1} exposed seedlings (Kumar *et al.*, 2013). The 80 µg. mL^{-1} exposure upregulated the expression level of miR169 and miR319, while 10 µg. mL^{-1} did not affect the expression patterns of these microRNAs. The miR397 expression level was increased in the seedlings by both concentrations. The expression of miR399 was not greatly affected in the seedlings by exposure to either of these two gold nanoparticle concentrations (Kumar *et al.*, 2013). The lower level of expression of miR398 and miR408 in gold nanoparticles exposed seedlings supported the elevation of antioxidant enzyme activity. These two microRNAs are also known to participate in the regulation of seed germination, seedling growth and root length. A lower level of expression of miR398 and miR408 may have been responsible for greater rate of seed germination, seedling growth and root elongation compared to control seedlings to that of the control indicating that these nanoparticles do affect the growth of the plants (Kumar *et al.*, 2013).

The gold nanoparticles can be used for nanoparticles mediated plant transformation in biotechnology and as capping agents to promote bio-safety and sensitivity (Saha *et al.*, 2012). AuNPs were used to cap mesoporous honeycomb silica nanoparticles to deliver plasmid DNA and its activators in a regulated manner (Torney *et al.*, 2007). The mesoporous silica nanoparticles were loaded estradiol to simultaneously deliver both DNA and effectors resulting in site targeted delivery and expression of chemicals and genes respectively in *Zea mays* and tobacco (Torney *et al.*, 2007).

UNIVERSITY of the WESTERN CAPE
https://etd.uwc.ac.za

2.3. Description of PEG and chitosan.

A polymer is a long-chain of repeating units (Kadajji and Betageri, 2011). The use of polymers in nanoparticles is due to ease of processing, their solubility and low toxicity and ability to control the growth (Usman *et al.*, 2012). Polymers are excellent stabilizing and capping agents for nanoparticles (Kadajji and Betageri, 2011). The poly (ethylene) glycol (PEG) is a water-soluble synthetic polymer while chitosan is a natural organic polymer extracted from crab shells, shrimps and fungi (Kadajji and Betaheri, 2011; Sharif *et al.*, 2018). The PEG is bio-adhesive and muco-adhesive (Kadajji and Betageri, 2011) and is also hydrophilic with high viscosity forming H-bonds (Özdemir and Güner, 2007). The PEG polymer is biocompatible with most organic solvents, non-immunogenic, non-antigenic and inhibits non-specific attachment of peptide and proteins (Alcantar, Aydil and Israelachvili, 2000). The chemical structure, $H–(O–CH_2–CH_2–)_m–OH$, of PEG consists of two terminal groups, hydrogen and hydroxyl, which play an important role in short compounds. Hydrophobic ethylene units and the hydrophilic oxygen which alternate along the chain are responsible for PEG's amphoteric character (Ozdemir and Guner, 2007). The one disadvantage of using PEG as stabilizing agent, site-specific delivery of proteins is its probability to aggregate other aqueous solutions. Synthetic polymers are degraded by simple hydrolysis, and the rate can be designed based on their molecular weight (Ozdemir and Guner, 2007). The polymer pathogen contamination is less in synthetic polymers than in natural polymers (Alcantar, Aydil and Israelachvili, 2000; Ozdemir and Guner, 2007).

UNIVERSITY of the
WESTERN CAPE

Chitosan is a chitin derivative possessing more than 50% degree of deacetylation (DDA (Aranaz *et al.*, 2014; Sharif *et al.*, 2018). Chitosan is non-toxic, biocompatible, and biodegradable and bioactive hence it is suitable for pharmaceutical, biomedical, food, biotechnological, agricultural and cosmetics applications (Usman *et al.*, 2012). Chitosan is a polysaccharide, with two monomeric units of 2-amino-2-deoxi-D-glucose linked by β (1→4) glycosidic bonds (Usman *et al.*, 2012). The solubility of chitosan is determined by amine group protonation of its copolymer structure (Aranaz *et al.*, 2014). The content of two amino-2-deoxi-D-glucose promotes its solubility in acidic aqueous solutions. Chitosan exists with positively charged structure capable of muco-adhesion, antimicrobial and permeability enhancing ability (Aranaz *et al.*, 2014).

https://etd.uwc.ac.za

Chitosan also has the ability to scavenge different radical species by either proton donation or electron transfer from the amine group (Aranaz *et al.*, 2014). Its cationic structure is great advantage for site-specific delivery of any specific anionic structure such as gold nanoparticles across membranes (Aranaz *et al.*, 2014). The major drawbacks of naturally occurring biopolymers are significant variations in molecular weight and structure from batch to batch, and the potential risk of pathogen transfer from the originating organism (Mignon, *et al.*, 2019). The structure of PEG and chitosan and are shown in **Fig.2** below, while their properties are compared in a summary in **Table 2:** below.

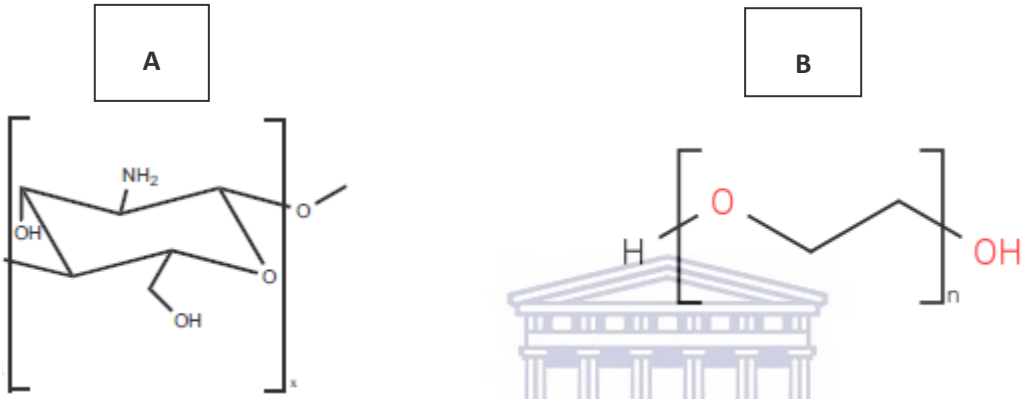

Figure 2: Chitosan and PEG structures. **A)** Chitosan (adapted from Aranaz *et al.*, 2014) **B)** PEG structure (adapted from Team, 2019).

UNIVERSITY of the
WESTERN CAPE

Table 2: Similarities and differences of chitosan and poly ethylene glycol (PEG).

Properties	Chitosan	Poly (ethylene) glycol (PEG)
Polymer classification	Natural biopolymer	Synthetic biopolymer
Solubility	Water soluble	Water soluble
Degradation	Hydrolysis, deacetylation	Hydrolysis
Structural Bonds	β-glycosidic bonds (1-4)	hydrophilic bonds
Biocompatible to cells	Highly	Highly
Immunogenecity	None	None
pathogenic contamination	High	Negligible
AuNPs stabilizing agent	Good stabilizing agents	Dependent on PEG molecular weight

https://etd.uwc.ac.za

In this work, the PEG and chitosan were used as stabilizers of the GYY4137 nanoparticles.

2.5. References

1. Alcantar, N. Avdil, E., Israelachvili T. (2000). Polyethylene glycol-coated biocompatible surfaces.*Journal of Biomedical Materials Research*, 51(3), pp. 343-351.
2. Aranaz, I., Mengibar, M., Harris, R., Miralles, B., Acosta, N., Calderon, L., Sanchez, A. and Heras, A. (2014). Role of Physicochemical Properties of Chitin and Chitosan on their Functionality. *Current Chemical Biology*, 8(1), pp.27-42.
3. Cabuzu, D., Cirja, A., Puiu, R. and Grumezescu, A. (2015). Biomedical Applications of Gold Nanoparticles. *Current Topics in Medicinal Chemistry*, 15(16), pp.1605-1613.
4. Daniel, M. and Astruc, D. (2004). Gold Nanoparticles: Assembly, Supramolecular Chemistry, Quantum-Size-Related Properties, and Applications toward Biology, Catalysis, and Nanotechnology. Chemical Reviews, 104(1), pp.293-346.
5. García-Mata, C. and Lamattina, L. (2012). Gasotransmitters are emerging as new guard cell signalling molecules and regulators of leaf gas exchange. *Plant Science*, 201-202, pp.66-73.
6. Huang, X., Jain, P., El-Sayed, I. and El-Sayed, M. (2007). Gold nanoparticles: interesting optical properties and recent applications in cancer diagnostics and therapy. *Nanomedicine*, 2(5), pp.681-693.
7. Jain, P., Lee, K., El-Sayed, I. and El-Sayed, M. (2006). Calculated Absorption and Scattering Properties of Gold Nanoparticles of Different Size, Shape, and Composition: Applications in Biological Imaging and Biomedicine. *The Journal of Physical Chemistry B*, 110(14), pp.7238-7248.
8. Judy, J. D., Unrine, J. M., Rao, W., Wirick, S., and Bertsch, P. M. (2012). Bioavailability of gold nanomaterials to plants: importance of particle size and surface coating. *Environmental Science and Technology*.46, 8467–8474.
9. Koelmel, J., Leland, T., Wang, H., Amarasiriwardena, D. and Xing, B. (2013). Investigation of gold nanoparticles uptake and their tissue level distribution in rice plants by laser ablation-inductively coupled-mass spectrometry. *Environmental Pollution*. 174, pp.222-228
10. Kumar, V., Guleria, P., Kumar, V. and Yadav, S. (2013). Gold nanoparticle exposure induces growth and yield enhancement in *Arabidopsis thaliana*. *Science of the Total Environment*, 461-462, pp.462-468.

UNIVERSITY of the
WESTERN CAPE
https://etd.uwc.ac.za

11. Mignon, A., De Belie, N., Dubruel, P. and Van Vlierberghe, S. (2019). Superabsorbent polymers: A review on the characteristics and applications of synthetic, polysaccharide-based, semi-synthetic and 'smart' derivatives. *European Polymer Journal*, 117, pp.165-178.
12. Milewska-Hendel, A., Zubko, M., Karcz, J., Stróż, D. and Kurczyńska, E. (2017). Fate of neutral-charged gold nanoparticles in the roots of the *Hordeumvulgare L*. cultivar Karat. *Scientific Reports*, 7(1).
13. Özdemir, C. and Güner, A. (2007). Solubility profiles of poly (ethylene glycol)/solvent systems, I: Qualitative comparison of solubility parameter approaches. *European Polymer Journal*, 43(7), pp.3068-3093.
14. Piella, J., Bastús, N. and Puntes, V. (2016). Size-Controlled Synthesis of Sub-10-nanometer Citrate-Stabilized Gold Nanoparticles and Related Optical Properties. *Chemistry of Materials*, 28(4), pp.1066-1075.
15. Sabo-Attwood, T., Unrine, J., Stone, J., Murphy, C., Ghoshroy, S., Blom, D., Bertsch, P. and Newman, L. (2011). Uptake, distribution and toxicity of gold nanoparticles in tobacco (*Nicotianaxanthi*) seedlings. Nanotoxicology, 6(4), pp.353-360.
16. Saha, K., Agasti, S., Kim, C., Li, X. and Rotello, V. (2012). Gold Nanoparticles in Chemical and Biological Sensing. *Chemical Reviews*, 112(5), pp.2739-2779.
17. Shah, V. and Belozerova, I. (2008). Influence of Metal Nanoparticles on the Soil Microbial Community and Germination of Lettuce Seeds. *Water, Air, and Soil Pollution*, 197(1-4), pp.143-148.
18. Sharif, R., Mujtaba, M., Ur Rahman, M., Shalmani, A., Ahmad, H., Anwar, T., Tianchan, D. and Wang, X. (2018). The Multifunctional Role of Chitosan in Horticultural Crops; A Review. *Molecules*, 23(4), p.872.
19. Siddiqi, K., Husen, A. (2016). Engineered gold nanoparticles and plant adaptation potential**.** *Nanoscale Research Letters*, 11(1). p. 400.
20. Taylor, A. F., Rylott, E. L., Anderson, C. W. N. & Bruce, N. C (2014) Investigating the Toxicity, Uptake, Nanoparticle Formation and Genetic Response of Plants to Gold. *PLOS ONE* .**9**, e93793.
21. Team, E. (2019). Poly (ethylene glycol) (CHEBI: 46793). [online] Ebi.ac.uk. Available at: https://www.ebi.ac.uk/chebi/searchId.do?chebiId=CHEBI:46793 [Accessed 14 May 2019].
22. Usman, M., Ibrahim, N., Shameli, K., Zainuddin, N. and Yunus, W. (2012). Copper Nanoparticles Mediated by Chitosan: Synthesis and Characterization via Chemical Methods. *Molecules,* 17(12), pp.14928-14936.

UNIVERSITY of the WESTERN CAPE
https://etd.uwc.ac.za

23. Torney, F., Trewyn, B., Lin, V. and Wang, K. (2007). Mesoporous silica nanoparticles deliver DNA and chemicals into plants. Nature Nanotechnology, 2(5), pp.295-300.
24. Wangoo, N., Kaur, S., Bajaj, M., Jain, D. and Sharma, R. (2014). One pot, rapid and efficient synthesis of water dispersible gold nanoparticles using alpha-amino acids. *Nanotechnology*, 25(43), p.435608.
25. Yeh, Y., Creran, B. and Rotello, V. (2012). Gold nanoparticles: preparation, properties, and applications in bionanotechnology. *Nanoscale*, 4(6), pp.1871-1880.
26. Zarabi, M., Arshadi, N., Farhangi, A. and Akbarzadeh, A. (2013). Preparation and Characterization of Gold Nanoparticles with Amino Acids, Examination of Their Stability. *Indian Journal of Clinical Biochemistry*, 29(3), pp.306-314.
27. Zhai, G., Walters, K., Peate, D., Alvarez, P. and Schnoor, J. (2014). Transport of Gold Nanoparticles through Plasmodesmata and Precipitation of Gold Ions in Woody Poplar. *Environmental Science & Technology Letters*, 1(2), pp.146-151.

UNIVERSITY of the
WESTERN CAPE

https://etd.uwc.ac.za

Chapter 3

Chapter Overview

This chapter contain methodologies used to synthesize GYY4137-capped gold nanoparticles (AuNPs), the capping with PEG and chitosan to make stable nanoparticles and characterization techniques used to study their physicochemical properties.

3. Method and Materials

3.1. Chemicals

Gold (iii) chloride hydrate ($HAuCl_{4.x}H_2O$, anhydrous 50% Au basis), L-serine (99.5%), L-threonine (99.5%), morpholin-4-ium 4-methoxyphenyl (morpholino) phosphinodithioate (GYY4137), poly (ethylene) glycol (PEG) (300 M_w), deacetylated chitin poly (D-glucosamine), acetic acid ($C_2H_4O_2$, 99-100%) and sodium tripolyphosphate (85%) ($Na_5O_{10}P_3$) were used. All the glassware used in the experiment was cleaned using aqua regia (1:3). Aqua regia is made up of one molar nitric acid (HNO_3) (65%) and 3 molar hydrochloric acid (HCl) (38%) to eliminate any metal contamination prior to use and stored overnight at 100^oC.

UNIVERSITY of the
WESTERN CAPE

The amino acids were purchased from Biochemika, acetic acid and nitric acid were products of Merk and all other chemicals from Sigma Aldrich (South Africa). The magnetic stirrers were sterilised with ethanol (99.9%) and washed with deionized water. The 0.01 (wt. %) of $HAuCl_4$, 300 mM GYY4137 and 300mM amino acids solutions were prepared with deionised water, Synthesis of AuNPs was done in the Nanomaterials and Organometallics Research Laboratory Chemical Science Building at the University of the Western Cape.

3.2. GYY4137, serine and threonine AuNPs synthesis.

The experimentation synthesized 20 mL of each solution of GYY4137-AuNPs, serine-AuNPs and threonine-AuNPs. In the experiments 10 mL of 0.01 wt. % $HAuCl_4$ was heated and refluxed in a 100-mL-round-bottom flask at 80 ^{o}C with continuous stirring according to the modified method of Wangoo *et al.*, 2014. While, heating a 10 mL of each 300 mM of the reducing agents (GYY4137, serine and threonine) were added to make three gold solutions. An observation of colour changes from yellow to purple, pink or brown solutions were observed. After which the reaction was cooled at room temperature with continuous

https://etd.uwc.ac.za

stirring. The solutions were stored in the dark away from direct light to avoid photo-induction.

3.2.1. GYY4137 AuNPs capping with PEG and chitosan.

GYY4137-AuNPs solutions of chloroauric acid solution (10 mL of 0.01 wt. %) was heated and refluxed in a 100-mL-round-bottom flask using at 80 ^{o}C with continuous stirring according to the modified method of Wangoo *et al.*, 2014. In the experiment 10 mL of 300 mM GYY4137 was added to10 mL of 0.1% $HAuCl_4$ boiled under reflux until colour change from yellow to ruby red. Thereafter, the reaction was cooled at room temperature with continuous stirring. In order to stabilize the GYY4137 AuNPs various concentrations (0.5%, 0.25%, 0.75%, 1% and 5%) of 10 mL PEG (300 $M_{w)}$ were added to the 10 mL 'GYY4137- AuNPs solutions at room temperature and stirred for 20 minutes to allow exchange of the GYY4137 molecules with PEG.

In order to produce0.2 % chitosan capped GYY4137 gold nanoparticles a 10 mL of 0.2% of deacetylated chitin poly glucosamine (chitosan) was dissolved in 1% acetic acid. Then a 10 mL solution of 0.1% GYY4137 and 0.1 % gold salt in a 1:1 ratio was added to the chitosan solution. Following this a 1mg/mL sodium tripolyphosphate (STTP) was added drop wise until a change yellow to transparent and to pink was observed in the solution. The mixture was stirred for 20 minutes and then sonicated for another20 minutes at room temperature. The solutions of the gold nanoparticles were subject to centrifugation at 6000 rpm for 30 minutes. The samples were stored away from direct light to avoid photo-induced reactions and analysed at room temperature with different techniques.

3.3. Characterization Of the gold nanoparticles.

3.3.1. Ultraviolet Visible (UV-Vis) spectroscopy

Using the Ultraviolet Visible (UV-Vis) spectroscopy surface plasmon resonance peak and the optical property of gold nanoparticle verification the formation of gold nanoparticles was performed. Double beam UV-Vis equipment was used. A two reference cells were used to calibrate then equipment prior to sample analysis, and then a sample cell was analysed in comparison to one reference cell. **Fig. 3:** The sample cell is put inside the UV-Vis equipment and UV beam passed through the sample and caused electrons in the sample to transition from lower orbital energy state to a high orbital energy (Chem.ucalgary.ca, 2019).

https://etd.uwc.ac.za

The energy changes gave absorbance on the structure of the molecule from comparing the light transmitted through the sample (I_s) and light through the reference (I_r) cell. The monochromator spreads the light into a spectrum and selects one wavelength of light that is split into two beams (Chem.ucalgary.ca, 2019). The sample absorbs light in the visible range of spectrum which gets detected by a detector. The UV-Vis was done in the Chemical Science Building in the Chemistry department.

This results in absorbance as equation:

$$\mathbf{A = \log\left(\frac{I_r}{I_s}\right) = \varepsilon bc}$$

Where **A**= Absorbance, $\mathbf{I_r}$= reference beam, $\mathbf{I_S}$= sample beam, **Ɛ** = molar absorptivity of the sample in$L.mol^{-1}.cm^{-1}$, **b**= path length in cm and **c** = concentration of sample in Molar.

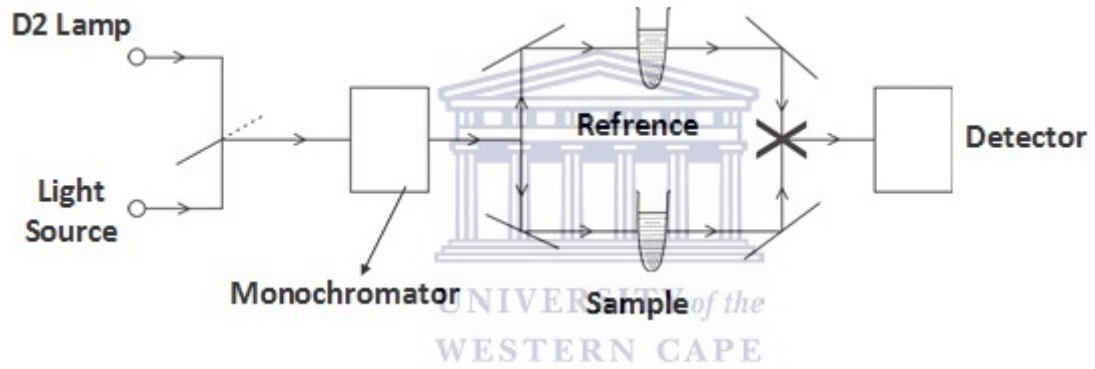

UNIVERSITY of the
WESTERN CAPE

Figure 3: Schematic diagram of double beam UV-Vis apparatus (adapted from: New Images Beam, 2019).

3.3.2. High resolution Transmission microscopy (HRTEM) analysis

Samples for HRTEM studies were prepared by dropping the nanoparticles solution on carbon-coated copper grids and were allowed to dry overnight minutes at room temperature before analysis. This technique gave the information of morphology of the gold nanoparticles. A FEI Tecnai^{TM} F30ST field emission gun transmission electron microscope (FEG-TEM) was operated at an accelerating voltage of 200 kV in bright field mode. In HRTEM, a high energy electron beam from an electron source focuses onto the sample and transmits the beam throughout the sample (Dstuns.iitm.ac.in, 2019). This beam results in changes in energy of electrons that can be detected by software and that generate an image of the sample (Dstuns.iitm.ac.in, 2019). HRTEM was performed in the physics department

https://etd.uwc.ac.za

at the Electron Microscopy Unit of University of the Western Cape. **Fig. 4:** Below is the example of an image of the HRTEM equipment with EDAX. Data analysis was done with Image J software to determine the size of the nanoparticles.

Figure 4: General layout of a HRTEM with EDAX (Dstuns.iitm.ac.in, 2019).

3.3.3. Energy dispersive X-Ray Analysis (EDX) analysis.

Energy dispersive X-Ray Analysis (EDX) is an elemental mapping of samples to approximately confirm the presence of the desired elements within the sample and any impurities thereof. The machine gives off the composition or number of nanoparticles near and at the surface, provided they contain some heavy metal ions. This technique was performed on samples after characterization with HRTEM. Upon exposure to the electron beam, the electrons within the sample were excited to a higher energy level, and released X-rays as they return to the ground state. The wavelength of each X-ray is unique to the element from which it was emitted. The EDS spectra were collected with liquid nitrogen cooled EDAX SiLi detector connected to the HRTEM. Each spectrum was collected for 30 seconds. The experiments were done in the Electron Microscopy Unit (EMU) in the physics department at the University of the Western Cape.

3.3.4 Scanning Transmission Electron Microscopy (STEM with EDAX)

In the scanning transmission electron microscopy (STEM) mode, the microscope lenses created focused convergent electron beam or probe at the sample surface. The focused probe

https://etd.uwc.ac.za

scanned across the sample and various signals are collected point-by-point to form an image (Nrel.gov, 2019). The analysis was done using a Zeiss Merlin FESEM with STEM detector and Smart SEM software to generate images. The samples quantified chemically using quantitative Energy Dispersive X-Ray Spectrometry (EDS) with using an Oxford Instruments® X-Max 20 mm^2 detector and Oxford Aztec software (Oxford Instruments, Oxfordshire OX13 5QX, United Kingdom). For Backscattered Electron detection (BSE), operating conditions of 20 kV accelerating voltage and 10 nÅ beam current with a working distance of 9.5 mm, were used. Beam conditions during the quantitative (EDS) analysis performed on the Zeiss MERLIN were 20 kV accelerating voltage, with a working distance of 9.5 mm and a beam current of 10 nÅ. The characterization happened in the University of Stellenbosch at the Central Analytical Facilities (CAF).

3.3.5. Attenuated Total Reflectance Fourier Transform Infrared spectroscopy (ATR-FTIR) analysis.

The use of polymers in the AuNPs requires confirmation that the polymers are linked to the surface of the AuNPs. Attenuated Total Reflection (ATR) is an accessory of transmission infrared (IR) spectrometers that significantly enhances surface sensitivity (Subramanian and Rodriguez-Saona, 2009). ATR probes substances to determine the nature of their molecular bonds and identifies the functional groups among organic molecules (Subramanian and Rodriguez-Saona, 2009). Only polar bonds display bands in the IR spectrum and are named IR active (Utdallas.edu, 2019).

Prior to the analysis, 99.9 % of acetone cleaned the ATR crystal and thereafter the background was analysed to ensure good results. A contact between ATR crystal and test sample of 80 to 100 gauge. ATR measured the changes that happened in an internally reflected infrared beam when the beam encountered a sample (Subramanian and Rodriguez-Saona, 2009). In ATR, an infrared beam is reflected internally through a crystal. In ATR-FTIR, as shown **in Fig. 5,** a crystal with high refractive index is placed underneath the sample. When IR radiation passes through the crystal, the total internal reflection takes place and generates an evanescent wave that is absorbed by the sample (Subramanian and Rodriguez-Saona, 2009). In this work, ATR- FTIR measurements were performed using ATR-FTIR spectra were recorded on a Perkin Elmer Spectrum 100 spectrometer in the

UNIVERSITY of the WESTERN CAPE
https://etd.uwc.ac.za

4000-500 cm^{-1} range. Data analysis was conducted with OMNIC Spectroscopy Software Suite. The analyses were done in the Chemistry department in the Chemical Science Building of University of the Western Cape.

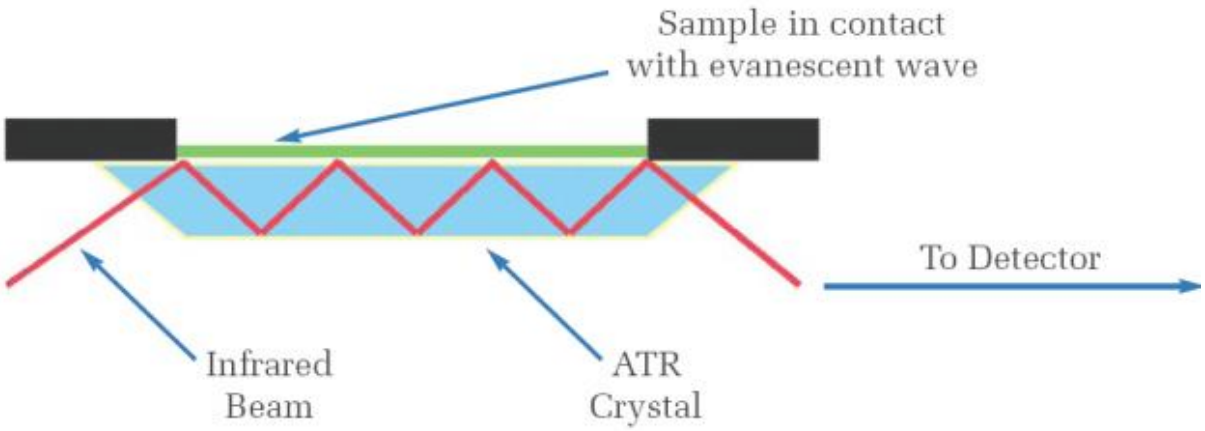

Figure 5: A Schematic representation of ATR-FTIR. Adapted from (Subramanian and Rodriguez-Saona, 2009).

3.3.6. Dynamic Light scattering and Zeta Potential

Dynamic light scattering (DLS) was used to determine the size of Brownian nanoparticles in colloidal suspensions in the ranges of nano and submicron (Stetefeld, McKenna and Patel, 2016). The Brownian motion results in Doppler shift when nanoparticles are exposed to a shining monochromatic light (laser) which hits the moving particle and resulting in changes in the wavelength of the incoming light (Stetefeld, McKenna and Patel, 2016). Degree of the change in wavelength determines the size of the particle (Kanjanawarut, Yuan and Xiao Di, 2013). Brownian motion assists in evaluation of the size distribution, particle's motion in the medium, which may further assist in measuring the diffusion coefficient of the particle and using the autocorrelation function (Kanjanawarut, Yuan and Xiao Di, 2013; Stetefeld, McKenna and Patel, 2016). DLS offers precise estimation of the particle diameter and size distribution (Stetefeld, McKenna and Patel, 2016). The instrument operates at a light source wavelength of 532 nm and fixed scattering angle of 73 ^{o}C over a 1 cm path length at room temperature (Stetefeld, McKenna and Patel, 2016).

The Zetaziser Nano ZS (Malvern Instruments, US) was used mean particle hydrodynamic size, size distribution and surface charge of the gold nanoparticles incorporated to a computer for data analysis. The Zetasizer Nano ZS was calibrated using dispersant of water prior to analysis. After that, one of the references was taken out and analysis began with one

UNIVERSITY of the WESTERN CAPE
https://etd.uwc.ac.za

reference cell and sample cell. Each data point for all measurements is an average of at least 10 runs. Each analysis time was for 60 sec. Zeta potential indicates the degree of repulsion for adjacent similarly charged particles and stability (Gupta, Singh and Singh, 2015). Zeta potential measurements are suitable for colloidal AuNPs because they possess a negative electrostatic charge. The surface charge of gold nanoparticles is pH dependent (Csapó *et al.*, 2014). The DLS and Zeta Potential measurements were done in the Life Science Building in the Biotechnology Department.

UNIVERSITY of the
WESTERN CAPE

https://etd.uwc.ac.za

3.4. References

1. Chem.ucalgary.ca. (2019). *Ch13 - UV-Vis Spectroscopy*. [online] Available at: http://www.chem.ucalgary.ca/courses/350/Carey5th/Ch13/ch13-uvvis.htmL [Accessed 16 May 2019].
2. Csapó, E., Sebők, D., MakraiBabić, J., Šupljika, F., Bohus, G., Dékány, I., Kallay, N. and Preočanin, T. (2014). Surface and Structural Properties of Gold Nanoparticles and Their Biofunctionalized Derivatives in Aqueous Electrolytes Solution. *Journal of Dispersion Science and Technology*, 35(6), pp.815-825.
3. Dstuns.iitm.ac.in. (2019). *High Resolution Transmission Electron Microscope (HRTEM) with EDAX*. [online] Available at: http://www.dstuns.iitm.ac.in/microscopy-instruments.php [Accessed 10 May. 2019].
4. Gupta, S., Singh, S. and Singh, R. (2015). Synergistic Effect of Reductase and Keratinase for Facile Synthesis of Protein-Coated Gold Nanoparticles. *Journal of Microbiology and Biotechnology*, 25(5), pp.612-619.
5. Kanjanawarut, R., Yuan, B. and XiaoDi, S. (2013). UV-Vis Spectroscopy and Dynamic Light Scattering Study of Gold Nanorods Aggregation. *Nucleic Acid Therapeutics*, 23(4), pp.273-280.
6. New Images Beam. (2019). *Single Beam And Double UV Visible Spectrometer - New Images Beam*. [online] Available at: http://www.fotoimage.org/single-beam-and-double-UV-Visible-spectrometer/ [Accessed 16 May 2019].
7. Nrel.gov. (2019). *Scanning Transmission Electron Microscopy | Materials Science | NREL*. [online] Available at: https://www.nrel.gov/materials-science/scanning-transmission.htmL [Accessed 6 Jun. 2019].
8. Stetefeld, J., McKenna, S. and Patel, T. (2016). Dynamic light scattering: a practical guide and applications in biomedical sciences. *Biophysical Reviews*, 8(4), pp.409-427.
9. Subramanian, A. and Rodriguez-Saona, L. (2009). Fourier Transform Infrared (FTIR) Spectroscopy. *Infrared Spectroscopy for Food Quality Analysis and Control*, pp.145-178.
10. Utdallas.edu. (2019). *INFRARED SPECTROSCOPY (IR): Theory and Interpretation of IR spectra*. [online] Available at: https://www.utdallas.edu/~scortes/ochem/OChem_Lab1/recit_notes/ir_presentation.pdf [Accessed 10 Jun. 2019].

https://etd.uwc.ac.za

11. Wangoo, N., Kaur, S., Bajaj, M., Jain, D. and Sharma, R. (2014). One pot, rapid and efficient synthesis of water dispersible gold nanoparticles using alpha-amino acids. *Nanotechnology*, 25(43), p.435608.

https://etd.uwc.ac.za

Chapter 4

Chapter overview

This chapter contains a brief discussion of the results of capped and uncapped GYY4137-AuNPs compared to serine-AuNPs and threonine-AuNPs with emphasis on the results obtained from all the characterization techniques employed to analyse the nanoparticles.

4. Results and Discussion

4.1. The formation of GYY4137-AuNPs, serine-AuNPs and threonine-AuNPs.

The GYY4137-AuNPs, serine-AuNPs and threonine-AuNPs were synthesised (**Fig.6**.) using GYY4137, serine and threonine as reducing agents. The novel GYY4137-gold nanoparticles resulted in a brown solution compared to serine–AuNPs (purple) while threonine-AuNPs (pink). Jain *et al.*, (2006) reported that spherical AuNPs exist as brown, purple or pink such as those obtained in this study.

The Ultra-Violet Visible spectroscopy verified the formation of the gold nanoparticles. In **(Fig. 7.)** GYY4137 –AuNPs had a surface plasmon resonance peak at 562 nm compared to serine gold nanoparticles and threonine gold nanoparticles which had 560 nm and 524 nm. All the nanoparticles absorbed in the visible range of the spectrum, which proved successful synthesis of the gold nanoparticles. The peak position and absorbance of the SPR band are dependent on AuNPs' size (Belahmar and Chouiyakh, 2016). The GYY4137 gold nanoparticles were relatively stable for few hours and required further stabilization before use with other characterization equipment. According to the Mie theory, the maximum absorption wavelength is related to the size of the nanoparticles and the smaller the wavelength, the smaller is the diameter of the nanoparticles (Saha *et al.*, 2012; Zarabi *et al.*, 2013). The observation of the broad absorbance peak of GYY4137 is indicative of large nanoparticles and shows signs of aggregation hence the use of chitosan polymer. While the serine-AUNPs and threonine-AuNPs had a narrower surface plasmon peak proving smaller diameter of nanoparticles and broad distribution size range shown by the broad-spectrum peak and wavelength. The serine-AuNPs agglomerated slowly than the threonine-AuNPs. The peak absorbance wavelength increases with particle size and localised surface plasmon resonance spectrum depends on diameter and shape of AuNPs (Zarabi *et al.*, 2013). The maximum absorbance peaks were determined to 524,550 and 562 nm reported to be

UNIVERSITY of the WESTERN CAPE

https://etd.uwc.ac.za

correlated with the size of 20 - 40nm of gold nanoparticles (Jain *et al.*, 2006). All the spectra had broad SPR peak in the spectrum, which showed the size distribution of polydispersed gold nanoparticles.

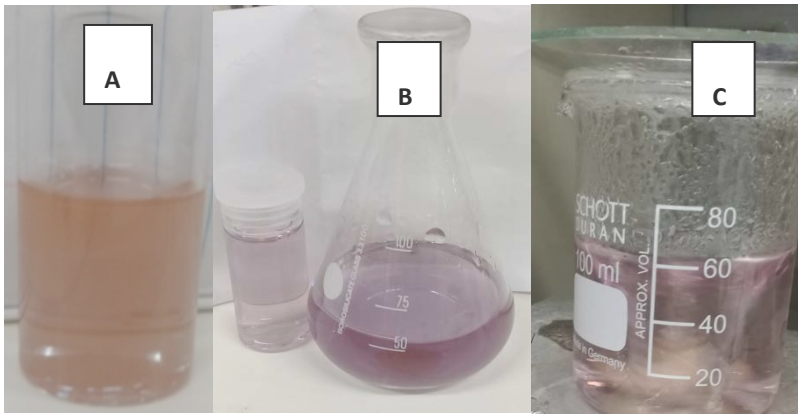

Figure 6: The synthesized samples of GYY4137-AuNPs compared to amino acid AuNPs. The beaker and conical flask **A) (**brown) GYY4137-AuNPs, **B)** (purple) serine-AuNPs and **C)** (pink) threonine-AuNPs.

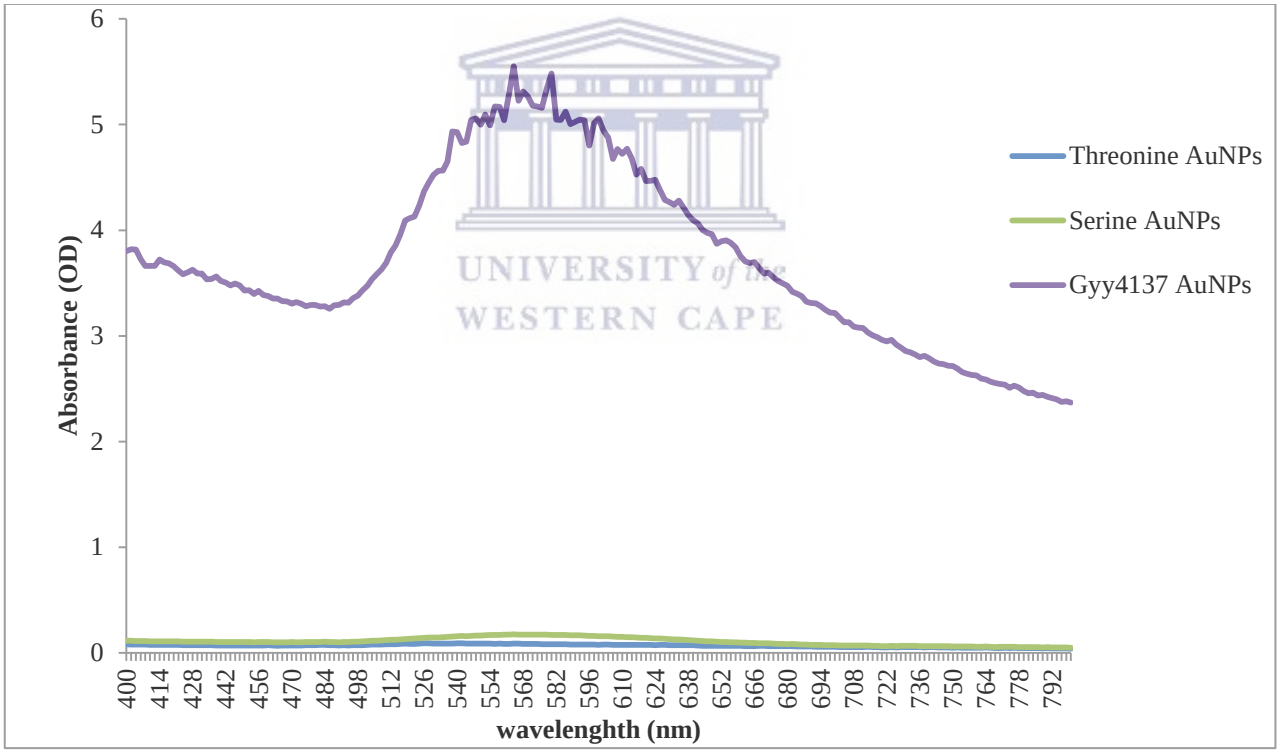

Figure 7: UV-Vis spectra of amino acids capped AuNPs and GYY4137-AuNPs. (Blue) threonine -AuNPs, (Green) Serine -AuNPs and (Purple) GYY4137 –AuNPs.

https://etd.uwc.ac.za

The band gap energy can be determined using the Tauc plot relation (Belahmar and Chouiyakh, 2016). It is an appropriate way of studying the optical absorption spectrum of a material (Belahmar and Chouiyakh, 2016). According to the Tauc relation, the absorption coefficient α for direct band gap material is given as (cited by Belahmar and Chouiyakh, 2016)

$(\alpha h\nu)^2 = A\,(h\nu - E_g)$

Where A is a constant**,** $\mathbf{E_g}$ is the optical band gap expressed in **eV** and **hν** is the photon energy in **eV** (Belahmar and Chouiyakh, 2016). The band gap value **(E_g)** is determined by using the linear part of the $(\alpha h\nu)^2$ curve towards the hν axis until $(\alpha h\nu)^2$ is zero (Belahmar and Chouiyakh, 2016). In (**Fig.8-10**) the obtained values of the optical band gap energy E_g are 2.10 eV, 2.07 eV and 2.1 eV for GYY4137-AuNPs, serine-AuNPs and threonine-AuNPs respectively. The $\mathbf{E_g}$ values increases as the size of the nanoparticle decreases. They decrease with the increase in fraction volume due to enlargement of nanoparticles size. The band gaps of the nanoparticles did not show the inverse relationship between the absorbance and band gap. As the band gap increases the absorbance of the nanoparticle decreases or vice versa. GYY4137-AuNPs and threonine-AuNPs had the same band gap although they absorbed at different maximum peak absorbance. The band gaps may show instability of the GYY4137-AuNPs and threonine-AuNPs compared to serine-AuNPs that had lower 2.07 eV band gap. Ashrafi (2011, p. 10) reported that band gap is dependent on size and shape of the nanoparticle and this relationship is due to electron quantum confinement at nanoscale referred to as quantum size effect (Ashrafi ,2011, p. 10).

UNIVERSITY of the
WESTERN CAPE

https://etd.uwc.ac.za

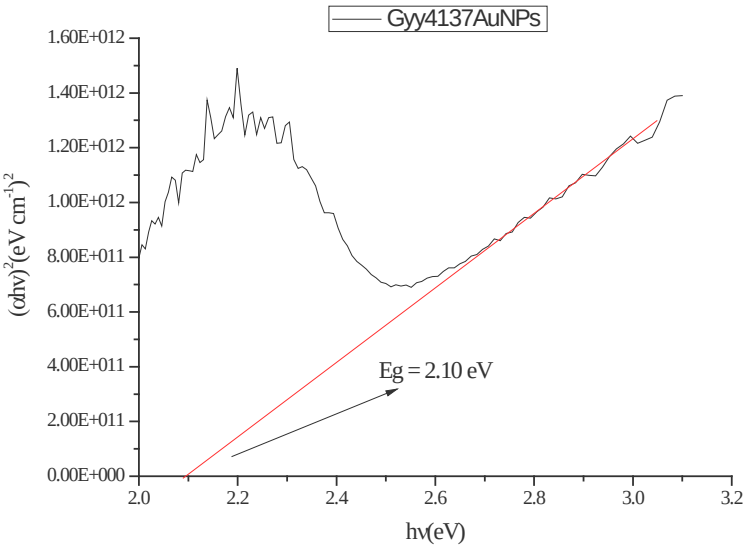

Figure 8: Tauc Plot of GYY4137-AuNPs with their band gap (E_g).

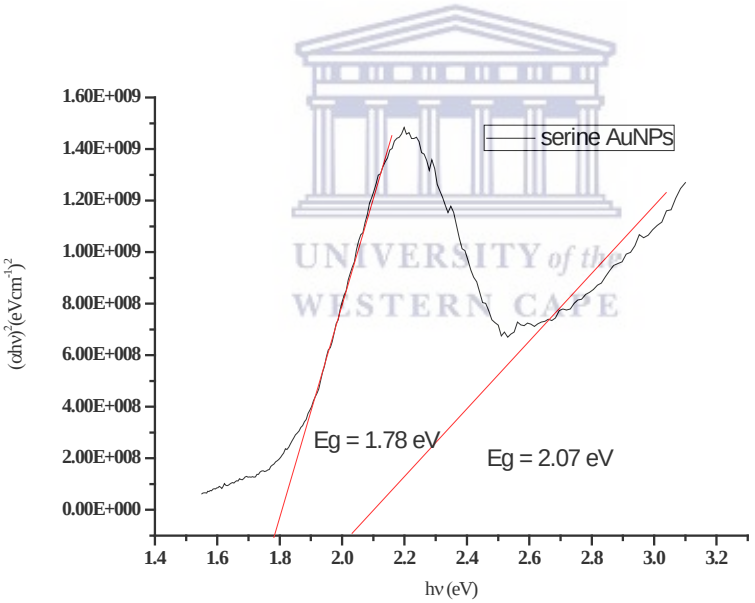

Figure 9: Tauc Plot of serine-AuNPs showing band gap (E_g).

https://etd.uwc.ac.za

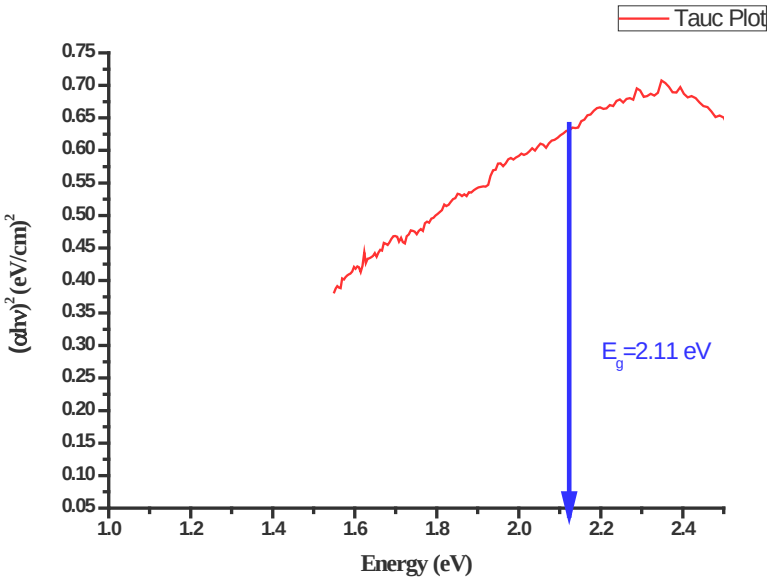

Figure 10: Tauc Plot of threonine-AuNPs showing band gap (E_g)

An aggregation results in the nanoparticles concentration decrease as the quality of nanoparticles deteriorated with time. The aggregation of AuNPs leads to an alteration in surface absorption band that gives rise to a visible colour change (Saha *et al.*, 2012). The GYY4137 AuNPs may have collapsed during synthesis or they were not encapsulated fully.

The concentration of the nanoparticles can be calculated from the Beer =Lambert law (A = εbC) using the molar absorptivity and the absorbance measured in UV−Vis spectra, where **A** is the absorbance, **b** is the path length of the sample (cm), **C** is the concentration of the compound in solution (mol. L^{-1}), and **ε** is the molar absorptivity (L mol^{-1} cm^{-1}). 4.2. PEG-capped GYY4137 AuNPs.

Coating of the nanomaterial surface has been shown to significantly alter nanoparticle absorption by the plant (Judy *et al.*, 2012)**.** In this study poly (ethylene) glycol (PEG) was used as a capping agent to stabilise GYY4147 because PEG can protect the chemical from outside environment and is biocompatible (Kadajji and Betageri, 2011). However, in our study none of the chosen concentrations (0.5-5%) of PEG could encapsulate the GYY4137 and in fact interfered with the whole synthesis procedure.

This may be because the effect of PEG on a biological sample is dependent on its concentration and its molecular weight of PEG (Zhu *et al.*, 2012). Hence, these concentrations of PEG did not stabilize the nanoparticles. Zhu *et al.*, (2012) has been

https://etd.uwc.ac.za

reported that high concentrations of PEG can result in drought stress induction in plant hence chitosan was used as an alternate polymer for capping. When the GYY4137-AuNPs were encapsulated with PEG brown solution appeared from concentration of 0.5 to 1. However, at 5% PEG a colourless solution was observed. The solutions did not show any spectra in the UV-Vis spectra proving unsuccessful synthesis of gold nanoparticles in the presence of PEG.

4.3. Characterization of chitosan capped GYY4137-AuNPs.

The techniques used to confirm the preparation of chitosan capped GYY4137-AuNPs compared to serine-AuNPs and threonine-AuNPs were ultra-violet visible spectroscopy (UV-Vis). Identification of the nanoparticle morphology, hydrodynamic size, size distribution, and surface charge was determined by High Resolution Transmission Electron Microscopy (HRTEM), Dynamic Light Scattering (DLS) and Zetasizer respectively. Attenuated Total Reflectance Fourier Transform infrared confirmed the structural encapsulation of the nanoparticles (ATR-FTIR).

(Fig.11.) Chitosan encapsulated the GYY4137-AuNPs and resulted in pink gold nanoparticle's solution. The colour change observed proved that gold nanoparticles formation was successful. The formation of the gold nanoparticles was verified with the absorption of UV-Vis **(Fig.12.)** of the chitosan capped GY4137-AuNPs with a maximum absorbance peak at 550 nm with an optical density of 0.29. The broadness of the maximum absorbance peak is indicative of broad size distribution of the nanoparticles. Chitosan decreased the absorbance surface plasmon resonance peak the GYY4137-AuNPs from 5.2 to 0.29 in the region of maximum wavelength from 562 nm to 550 nm compared to the preliminary results of the relatively stable GYY4137 AuNPs. There is a direct relationship between absorbance of the gold nanoparticles the size of the nanoparticles (Zarabi *et al.*, 2013). Absorbance increases as the size also increases and vice versa. **Table 3:** below shows the calculated concentration of the gold nanoparticles with their probability of aggregation and dispersity of the GYY4137 has significantly high concentration (3.2484) when compared to the preliminary studied serine-AuNPs and threonine-AuNPs. **(Fig.13.)** The presence of chitosan resulted in a band gap of the GYy4137-AuNPs of 1.7 eV and 2.0 eV. The $\mathbf{E_g}$ values show that as the band gap increases as the size of the nanoparticle decreases. This is agreement with the lower maximum absorbance peak of the nanoparticle in its UV-Vis spectrum.

UNIVERSITY of the WESTERN CAPE

https://etd.uwc.ac.za

Table 3: Concentration of the gold nanoparticles from Beer's law (A=Ɛbc)

AuNPs	**Absorbance (A) (OD)**	**Molar absorptivity (Ɛ)** **(L mol^{-1} cm^{-1})**	**Path length (b) cm**	**Concentration (c) (mol/L)**
L-Serine-AuNPs	**0,173**	**$7.70x\ 10^{10}$**	**1**	**0.02247**
L-threonine-AuNPs	**0,089**	**$9.21x\ 10^{8}$**	**1**	**0,00966**
GYY4137-AuNPs	**5.1**	**$1.57\ x\ 10^{11}$**	**1**	**3.2484**

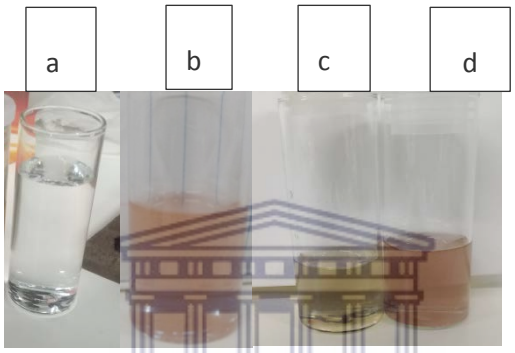

Figure 11: Colloidal solutions of chitosan capped GYY4137-AuNPs and uncapped GYY4137-AuNPs with precursor solutions**. (a)** GYY4137, **(b)** GYY4137-AuNPs, **(c)** $HAuCl_4^-$, **(d)** chitosan capped GYY4137-AuNPs.

UNIVERSITY of the
WESTERN CAPE

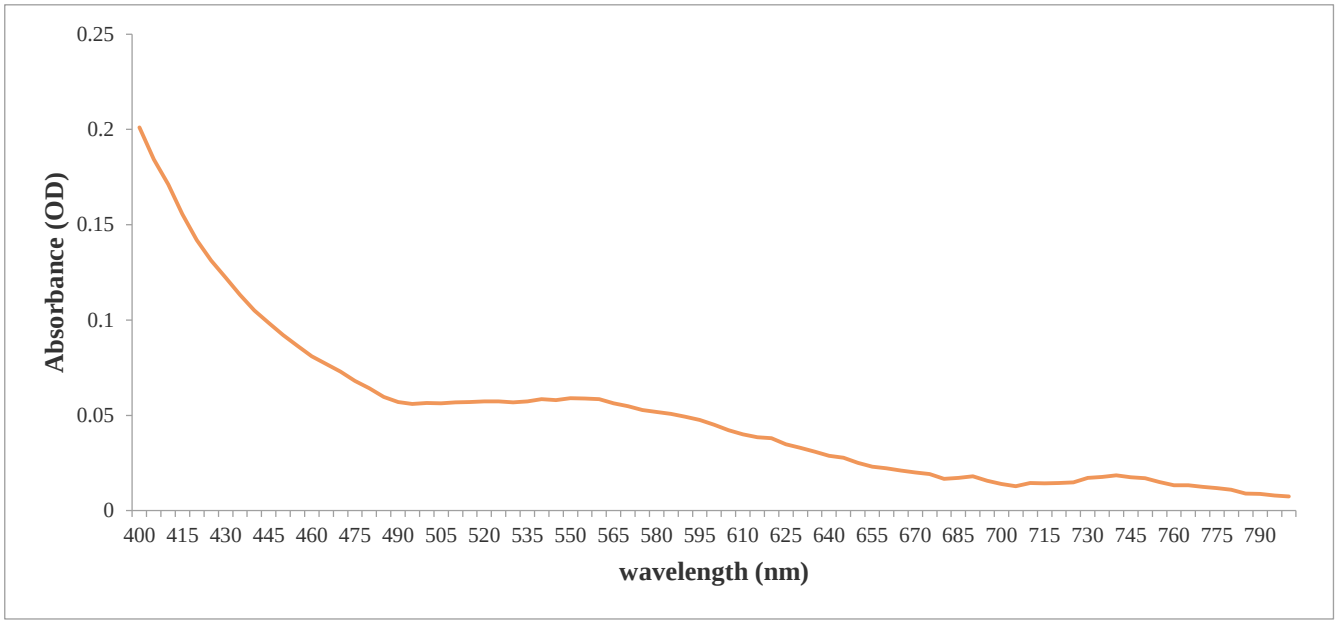

Figure 12: UV-Vis spectrum of chitosan capped GYY4137-AuNPs.

https://etd.uwc.ac.za

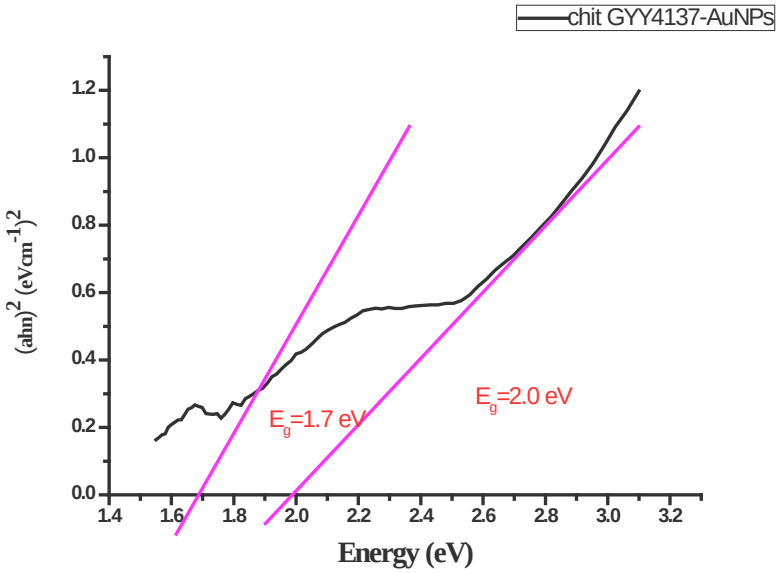

Figure 13: Tauc Plot of chitosan capped GYY4137-AuNPs showing band gap (E_g).

UNIVERSITY of the WESTERN CAPE

4.3.1. Functional groups of chitosan capped GYY4137-AuNPs.

(Fig. 14) below depicts the ATR-FTIR spectra of the reducing agents and gold salt: **(blue)** gold **(orange)** serine, **(grey)** threonine and (**yellow**) GYY4137 prior synthesis. The GYY4137 had one band in the analysis region of the spectra and a series found in the fingerprint region. The GYY4137 had one IR band of 3307.21 cm^{-1} and others in the finger print region of 611.08, 590.34, 574.23, 536.89, 520.50, 501.32, 483.26, 466.83 and 429.88 cm^{-1}.

The gold salt solution FTIR (ATR cm^{-1}) showed IR bands at 3276.08 cm^{-1}, 1635.09 cm^{-1}, 1066.13 cm^{-1}, 632.04 cm^{-1} and 420.52 cm^{-1}. The pure serine had 3325.74cm^{-1}, 1635 cm^{-1} and 579 cm^{-1}, threonine 3307.81cm^{-1}, 1636.20cm^{-1} and 576.01cm^{-1}. As the L-amino acids both have amides thus, N-H group is present in the 3000-3500 cm^{-1} region and a carbonyl group is present in the region of 1630-6600 cm^{-1}. These are showed by the strong polar O-H bond 3325.74 $cm^{-1}$and medium polar C =O bond 1635.33cm^{-1} for serine and 3307.81cm^{-1} and 1636.20 $cm^{-1}$for threonine and strong C-H bonds at the fingerprint region.

https://etd.uwc.ac.za

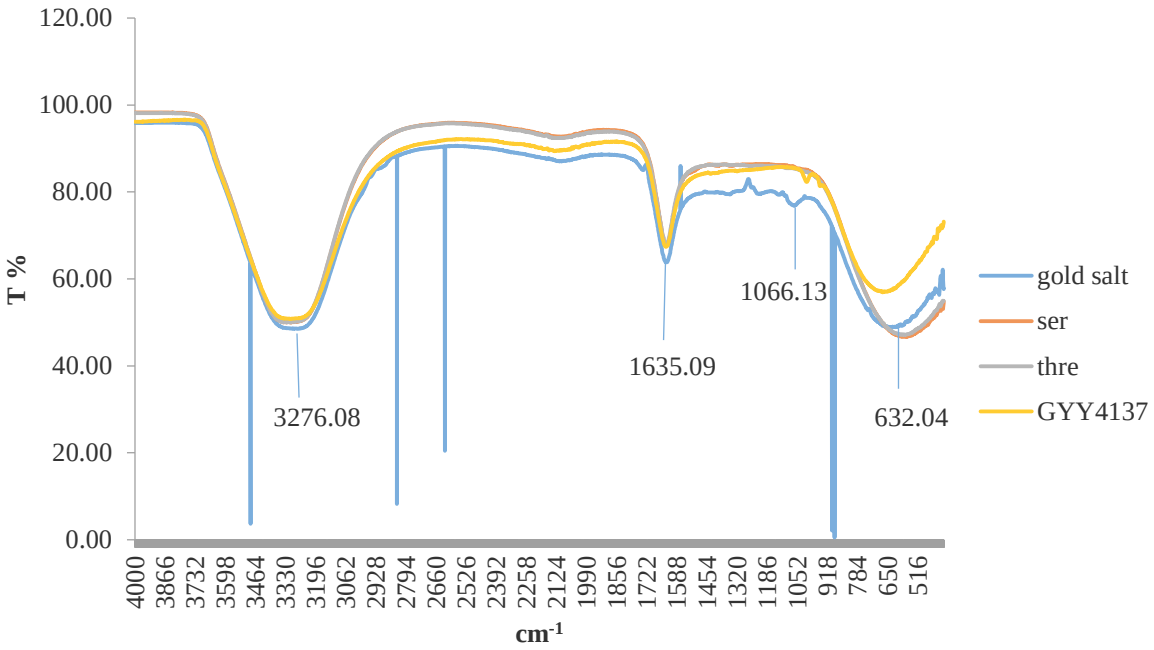

Figure 14: ATR-FTIR spectrum of all the reducing agents and gold salt solution prior to synthesis.

Figure 15 (a-c) below depicts the obtained ATR-FTIR spectra of chitosan capped GYY4137-AuNPs compared to serine-AuNPs and threonine-AuNPs. The chitosan capped GYY4137-AuNPs showed vibration bands at 3307.47, 2543.64, 2109.37, 1853.07 and 1636.82 cm^{-1}. The pure chitosan had bands at 3307.30 cm^{-1}, 1635.47cm^{-1}, 1272 cm^{-1}, 607 cm^{-1} and 422 cm^{-1}. In FTIR spectrum chitosan GYY4137-AuNPs capping with chitosan a slight shift of bands occurred from 3307.47 cm^{-1} to 3307.30 cm^{-1}, 1636.82 cm^{-1} to 1636.47 cm^{-1}, 1853.07 cm^{-1} to 1272.39 cm^{-1}. Two IR bands in the spectrum disappeared (2543.64 cm^{-1} and 2109.37 cm^{-1}) and two new ones appeared at 607 cm^{-1} and 422 cm^{-1}. The shift proved that chitosan really capped GYY4137-AuNPs. The relatively unstable GYY4137-AuNPs had a shift at absorption bands of 3307.21 cm^{-1} to 3306.82, 25 cm^{-1} and at 611.08 cm^{-1} to 672 cm^{-1}. New bands formed at 2548.71 cm^{-1}, 2132.21 cm^{-1}, 1854 cm^{-1}, 1636.53 cm^{-1}, 1223.63 cm^{-1}, 1010.48 cm^{-1} and 982 cm^{-1} (data not shown).

In comparison to serine-AuNPs with band at 3305.66 cm^{-1}; 2545.42 cm^{-1}; 2109.33 cm^{-1}; 1857.11 cm^{-1}, 1635.87 cm^{-1} and threonine-AuNPs at 3305.62, 2557.64, 2108.40, 1855.80 and 1636.68 cm^{-1}. The reduction of gold salt by the amino acids observed as small shift from 3305.74 cm^{-1} to 3325.66 cm^{-1}, and 1635.33 cm^{-1} to 1635.87 cm^{-1}. The 579.44 cm^{-1} band disappeared and new bond at 664.65 cm^{-1} with others 2545.42 cm^{-1}, 2109.33 cm^{-1}, 1857.11 cm^{-1} and 1156.93 cm^{-1} formed. The new bands formation shows that new bonds are formed between the reducing agents and the precursor gold salt solution.

https://etd.uwc.ac.za

All the gold nanoparticles have the same type regions of vibration as medium C=O stretch at 1636. 82 cm^{-1}; 1635.87 cm^{-1} and 1636.68 cm^{-1} respectively. They also have a strong bond at 3307.47 cm^{-1}; 3305.66 cm^{-1} and 3305.62 cm cm^{-1} belonging to the N-H stretching vibrations of amino groups of the amino acids. The weak C-H stretch observed at 2543.65 cm^{-1}, 2545.42 $cm^{-1}$and 2557.64cm^{-1} of methyl groups. The vibration bands of 1853.07 cm^{-1}1857.11cm^{-1} and 1855.80is the place region C-N stretch from the amine group bonds. Since gold and chloride are non-polar their bands are not shown in the FTIR but it is safe to say presence of symmetric C-H stretch (2543.64 cm^{-1}), C-C alkyne stretch (2109.37 cm^{-1}), C=C stretch (1853.07 cm^{-1}) and aromatic ring C=C 1636.82 cm^{-1} confirm the presence of gold nanoparticles as with amino acid AuNPs. Both serine and threonine possess polar uncharged side chains, amine bond and carbonyl (COO-H) bond they have approximately the same type of bonds and hence the more or less same vibrational regions.

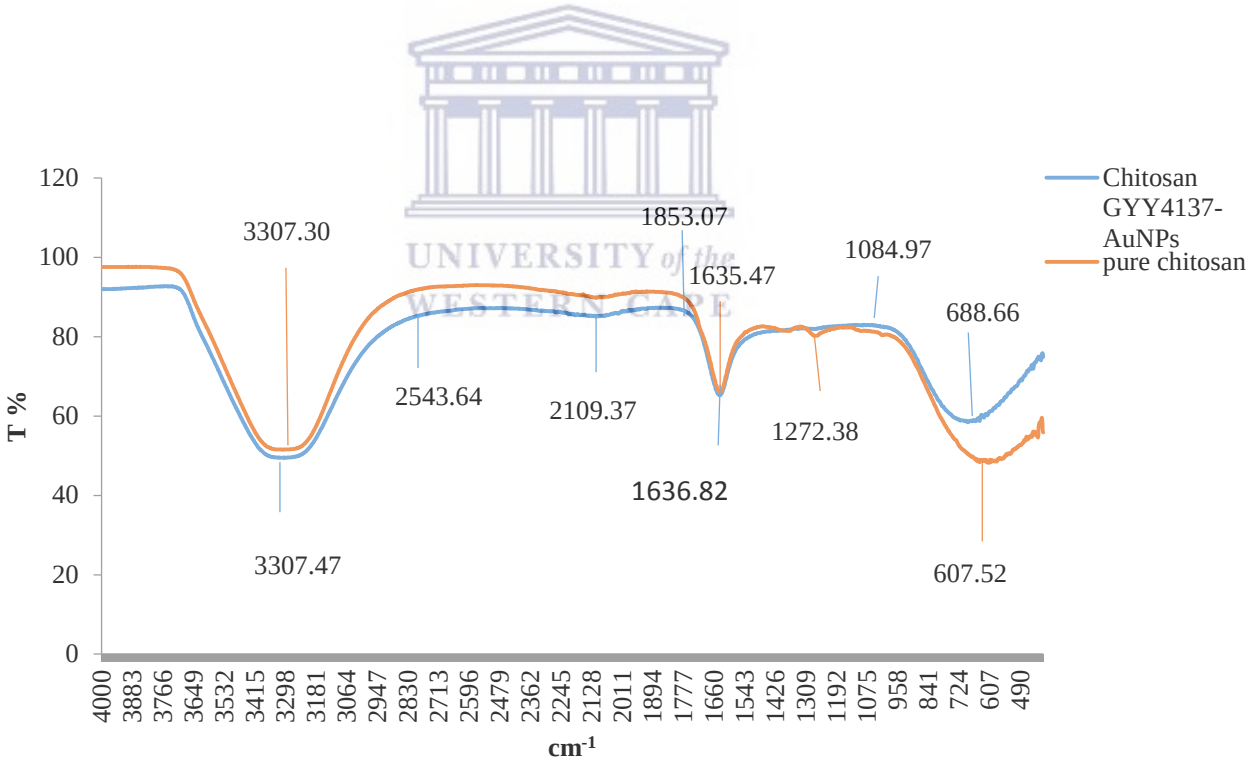

Figure 15 a: Pure chitosan and chitosan capped GYY4137-AuNPs as per ATR-FTIR image. **(orange)** Pure chitosan and **(blue)** chitosan capped GYY4137-AuNPs.

https://etd.uwc.ac.za

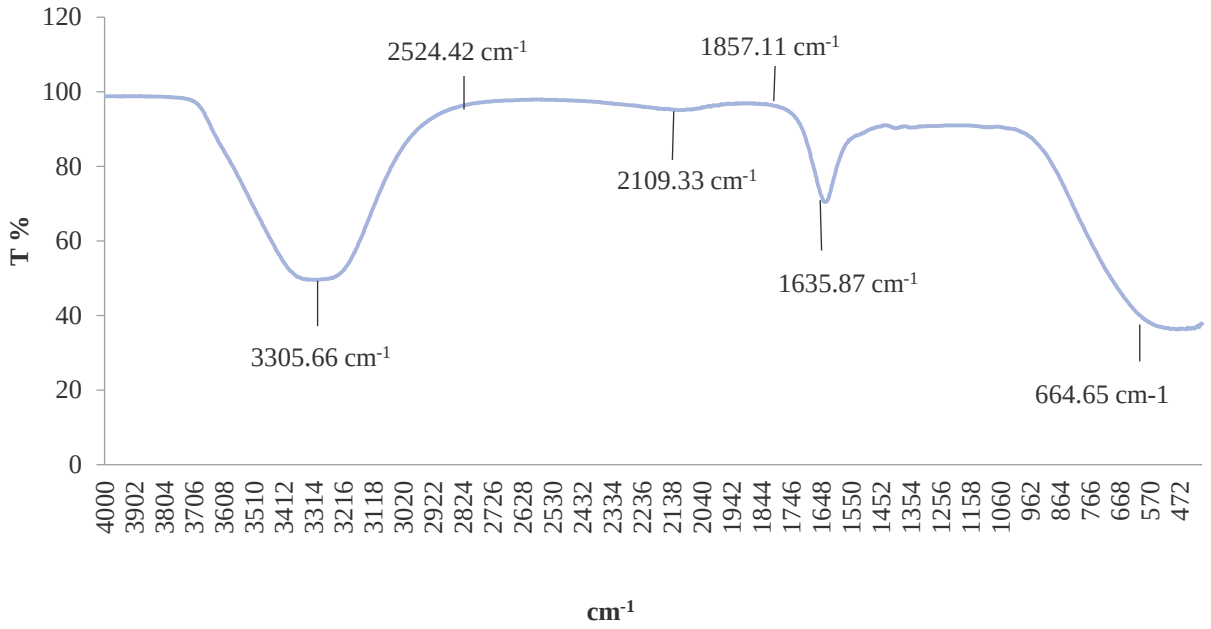

Figure 15 b: L-serine-AuNPs as per ATR-FTIR image.

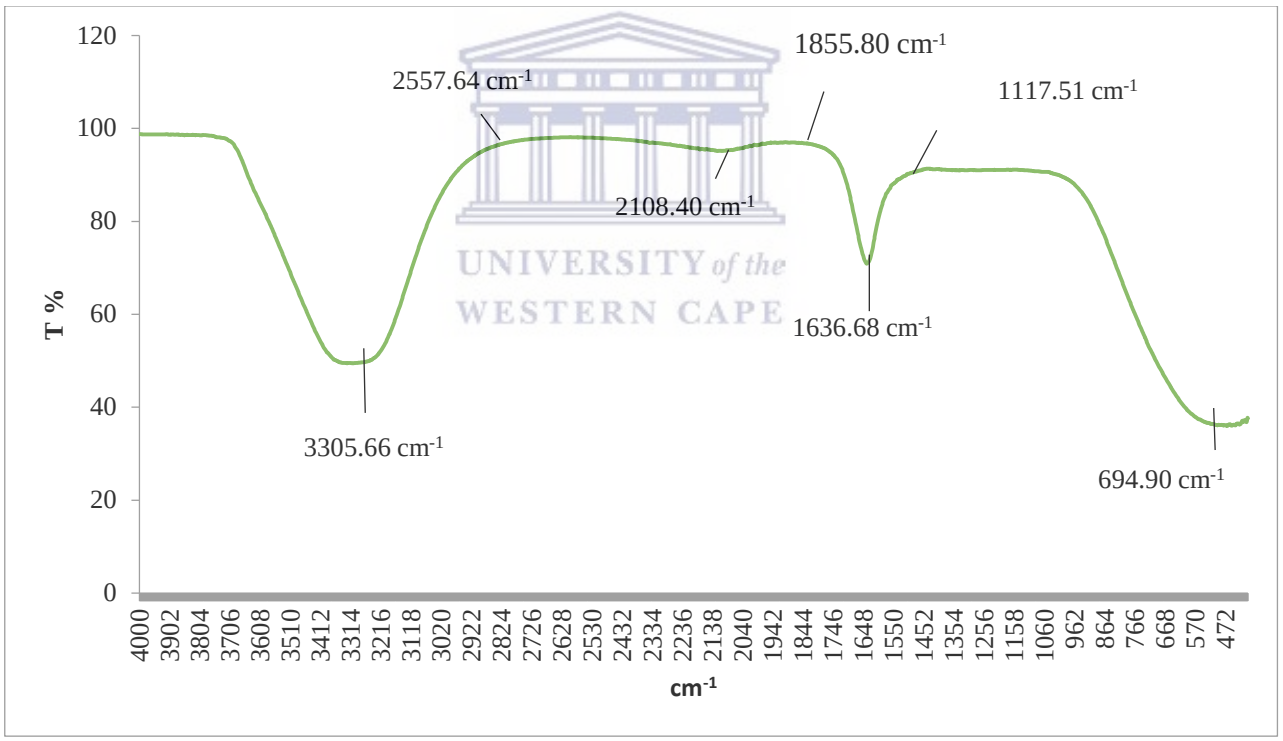

Figure 15 c: L- threonine AuNPs as per ATR-FTIR image.

https://etd.uwc.ac.za

4.3.2. The hydrodynamic size and size distribution of chitosan capped GYY4137-AuNPs.

The hydrodynamic sizes of the gold nanoparticles were measured by Dynamic Light Scattering (DLS) using Zetasizer Nano Series-Nano ZS (Malvern Instruments). The mean particle size as well as the polydispersity index (PDI), was evaluated with 10 runs. **(Fig.16 (a-c))** Dynamic light scattering revealed a mean particle size of 347 nm for chitosan capped GYY4137-AuNPs and a PDI of 0.357. Meanwhile both serine-AuNPs and threonine-AuNPs had different hydrodynamic size of 110.1 nm and 102 nm respectively and PDI of 0.406. The PDI of all the AuNPs proved that the nanoparticles had broad size range from all the reducing agents. This analysis also agreed with the UV-Vis results that all the nanoparticles had broad surface plasmon peaks. According to Tantra, Schulze and Quincey, (2010) PDI is a dimensionless measure of the broadness of the size distribution. The PDI exist between 0 and 1 and 0.1 PDI represents monodispersed nanoparticles. Values more than 0.1 indicate polydispersed nanoparticles in the sample and values between 0.1 and 0.25 are indicative of a narrow size particle distribution (Tantra, Schulze and Quincey, 2010). All the synthesized gold nanoparticles were polydisperse nanoparticles.

UNIVERSITY of the WESTERN CAPE

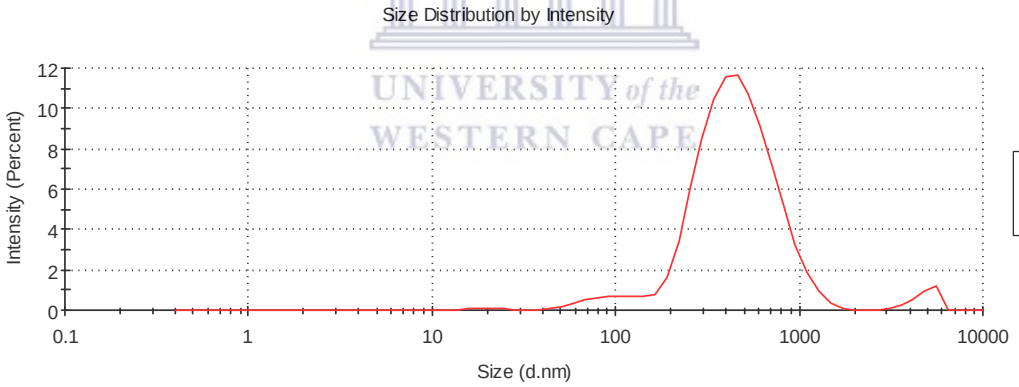

A

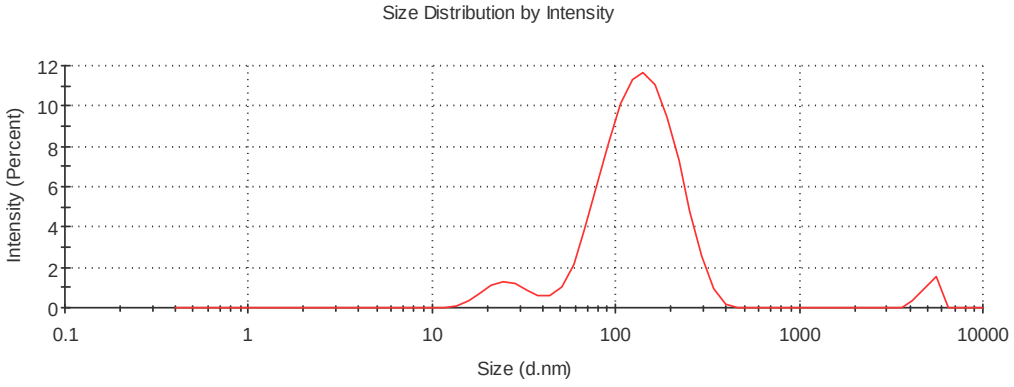

B

https://etd.uwc.ac.za

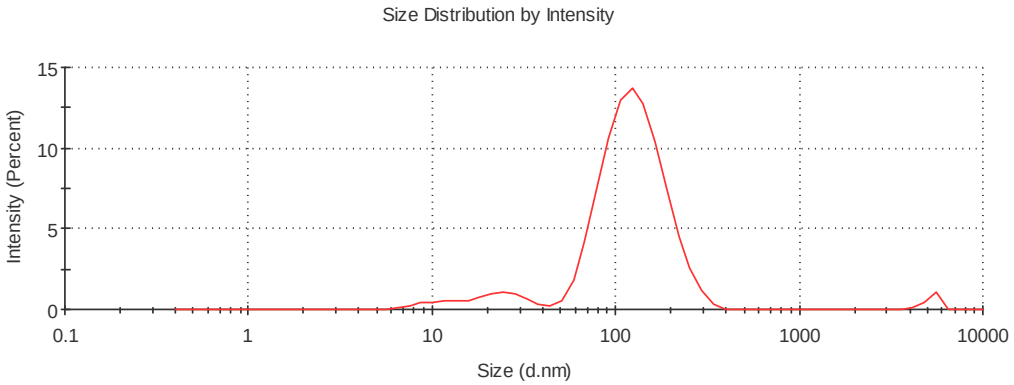

Figure 16: Graph of DLS measurements of GYY4137 AuNPs compared to L-serine gold nanoparticles and threonine AuNPs. **a**) GYY4137 AuNPs DLS, **b)** threonine AuNPs DLS, and **c)** serine AuNPs.

4.3.3. Surface charge (Z) of the chitosan capped GYY4137-AuNPs.

The surface charge (Z) of the gold nanoparticles was measured by zeta potential using Zetasizer Nano Series-Nano ZS (Malvern Instruments) in 10 run measurements. **(Fig.17)** The surface charge on chitosan capped GYY4137 AuNPs was + 47.8 mV. Zeta potential displays dispersity of nanoparticles or the coating of the nanoparticles surface with chitosan. The stability of different bio-functionalized AuNPs depends on temperature, pH, electrolyte concentration, biomolecule/gold nanoparticles ratio, reaction time, etcetera (Csapó *et al.*, 2014). Generally gold nanoparticles are negatively charged, but covering them with a polymer conferred them excellent stability and positive charges (Yeh,Creran and Rotello, 2012). For stabilized particles, the zeta potential is a measure of the particle's stability. Typically, nanoparticles with zeta potentials greater than 20 mV or less than -20mV have sufficient electrostatic repulsion to remain stable in solution (Keshvari, Bahram and Farshid, 2015).

In comparison to the surface charges of both serine-AuNPs (-2.91 mV) and threonine-AuNPs (-2.30 mV), GYY4137 had stable gold nanoparticles that could be used on biological samples this conferred by the presence of chitosan. Gupta, Singh and Singh, (2015) reported that zeta potential of -30 mV is vital for good stability and greater than -60 mV is excellently stable. The chitosan capped GYY4137 gold nanoparticles had good stability than both serine-AuNPs and threonine-AuNPs. The positively charged AuNPs those were stable for more than 30 days. These positively charged chitosan GYY4137 AuNPs were suitable for application to plants and investigation for bioaccumulation in plants since chitosan is biocompatible.

UNIVERSITY of the WESTERN CAPE
https://etd.uwc.ac.za

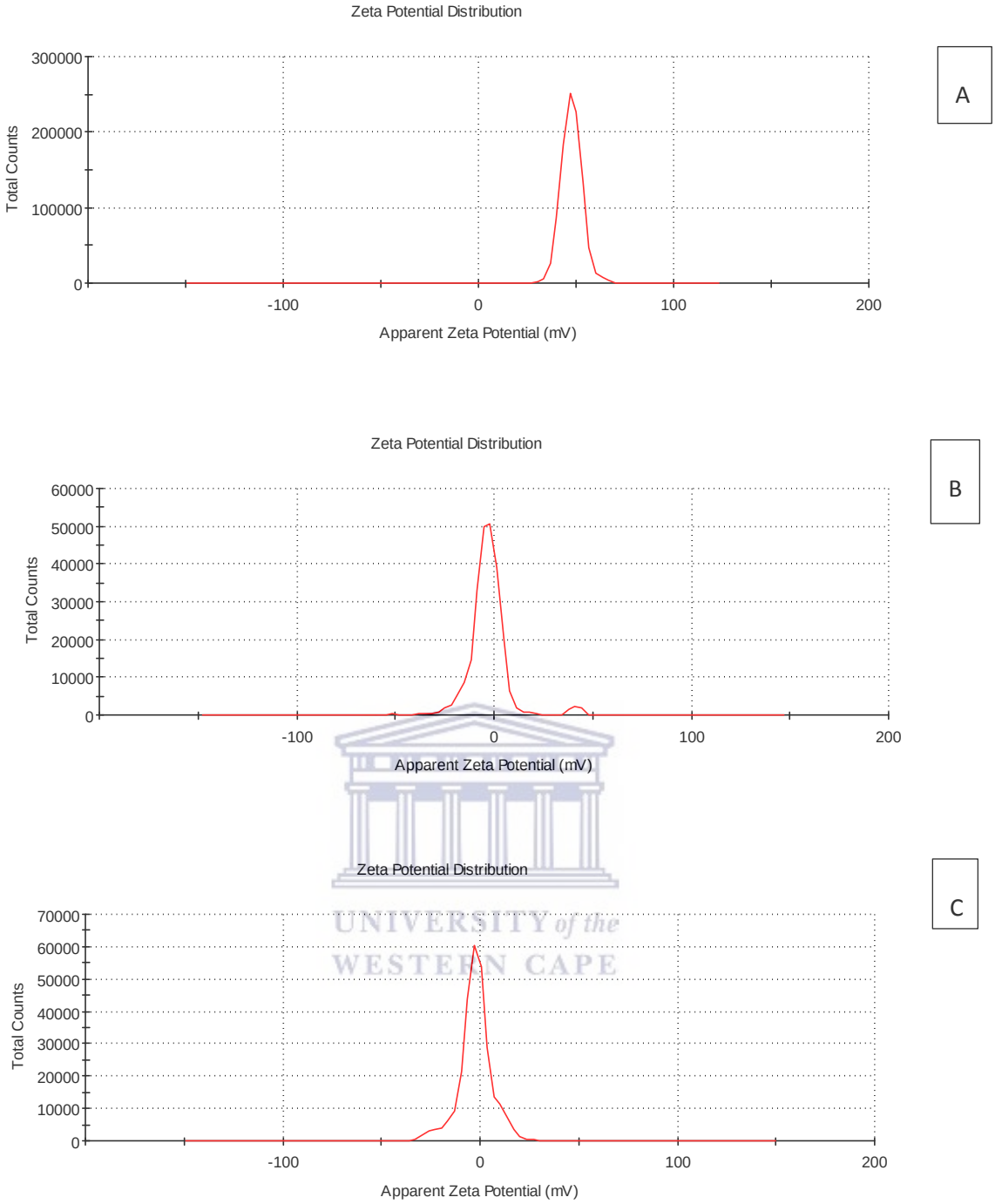

Figure 17: Graph of surface charge (Z) measurements of GYY4137-AuNPs compared to serine synthesized gold nanoparticles and threonine AuNPs. **a)** GYY4137-AuNPs, **b)** serine-AuNPs and **c)** threonine-AuNPs

4.2.6. Morphology of chitosan capped-GYY4137–AuNPs.

High Resolution Transmission electron microscopy (HRTEM) (**Fig. 18 (a-c))** shows micrographs obtained from the HRTEM of chitosan GYY4137-AuNPs (**a**) compared serine-AuNPs **(b)** and threonine-AuNPs **(c).** The GYY4137-AuNPs produced poly dispersed

https://etd.uwc.ac.za

icosahedral, spherical and tetrahedron shaped gold nanoparticles. While, the serine-gold nanoparticles consisted of spherical morphology and the threonine-AuNPs were highly agglomerated the morphology could not be obtained **(fig. 19-20)**. The HRTEM of the chitosan capped GYY4137-AuNPs was done after one month and 9 days of the synthesis this showed that the chitosan was really successful in encapsulating the gold nanoparticles and improving their stability. This proved that the nanoparticles were stable for more than 30 days.

The size distribution was between 20 and 180 nm in HRTEM. Most nanoparticles had a size of 100 nm and 140 nm. However, 100 nm is the highest of the nanoparticles size it is safe to assume chitosan capped GYY4137-AuNPs produce 100 nm. While in STEM micrographs the size of the chitosan capped GYY4137-AuNPs were 60 nm with the distribution of the nanoparticles between 20-80 nm a few of 140 nm. Serine-AuNPs had diameter of 60 nm as the chitosan GYY4137-AuNPs.

UNIVERSITY of the
WESTERN CAPE

https://etd.uwc.ac.za

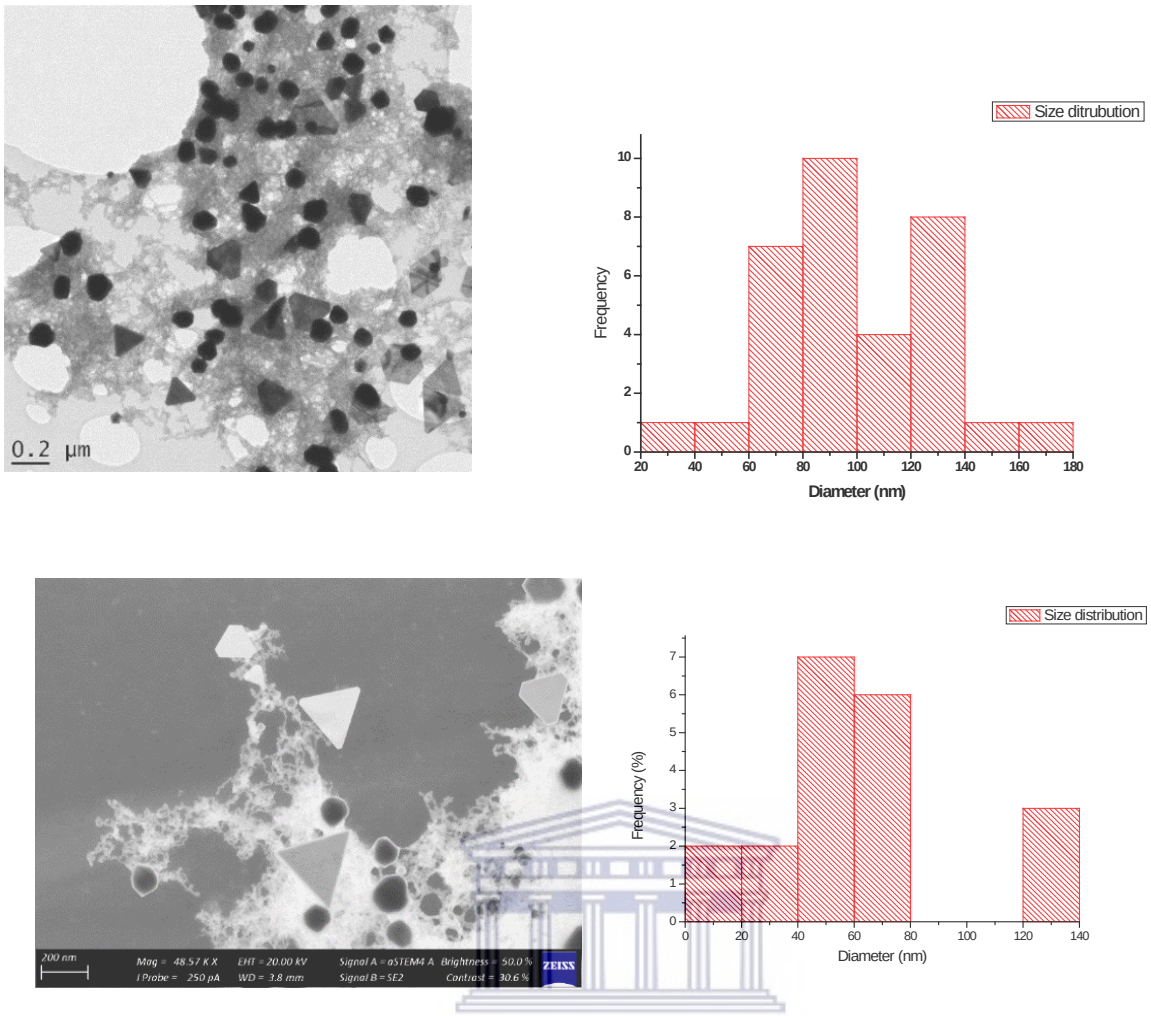

Figure 18: Micrographs of chitosan capped GYY4137-AuNPs and size distribution curve as per HRTEM and STEM. **(a)** Chitosan capped-GYY4137AuNPs at 0.2µm HRTEM. **(b)**Size distribution of chitosan-capped gold nanoparticles (HRTEM), **c)** chitosan STEM image at 200 nm, **d)** size distribution as per STEM image.

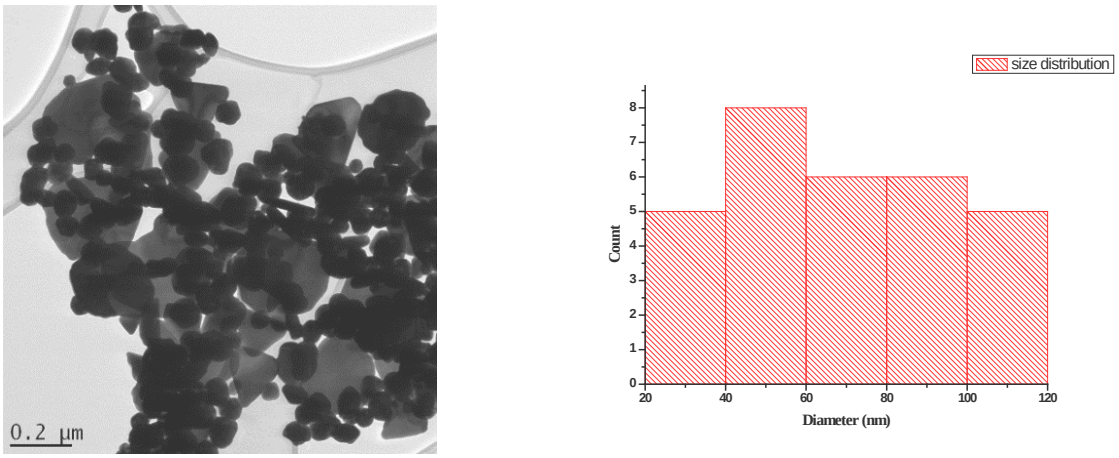

Figure 19: Morphology of serine-AuNPs and distribution curve as per HRTEM image.

https://etd.uwc.ac.za

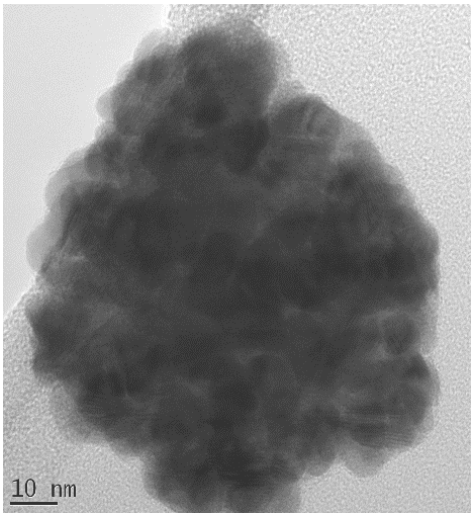

Figure 20: Morphology of threonine-AuNPs as per HRTEM image.

4.2.8. Elemental mapping of chitosan capped GYY4137-AuNPs.

The Energy Dispersive X-ray (EDX) gives the map of the compositional elements that are present in nanoparticles to confirm the gold nanoparticles presence. (**Fig. 21 (a-c))** The GYY4137-AuNPs showed elements of gold (Au), carbon (C), aluminium (Al), oxygen (O) and copper (Cu) compared to serine-AuNPs and threonine-AuNPs which had element of carbon (C), copper (Cu) and gold (Au). The carbon (C) and Cu are from the analytical instrument and Au is representative of successful gold nanoparticles presence in the samples. The presence of Au at 100,200, 500, 1100, and 380 counts at kilovolts from 1-15 KeV in the chitosan capped GYY4137-AuNPs and compared to serine-AuNPs and threonine-AuNPs have with the huge overlapping peaks at 1100 and 500 counts confirms the successful synthesis of the gold nanoparticles. The observed Cu is from the equipment as he and co-workers do not take it into account during calculations of w% (Składanowski *et al.*, 2016). Below is **(Table 4)** with the spectrum elements and their weight percentage (wt %). The EDX Au weight percentage of chitosan capped GYY4137-AuNPs was 48.56 % which is less than of Składanowski *et al.*, (2016) who had confirmed our serine-AuNPs and threonine-AuNPs EDX to have a wt% mass of Au of 84.8 % with the same position of Au in the EDX.

UNIVERSITY of the WESTERN CAPE

https://etd.uwc.ac.za

Table 4: Elements of chitosan capped GYY4137-AuNPs and their elements weight percentage from STEM-EDX images.

Spectrum Elements	Spectrum weight %
C	3.55
O	3.97
Mg	0
Al	3.36
Si	0
Cu	10.56
Au	48.58
Total	100

UNIVERSITY of the
WESTERN CAPE

https://etd.uwc.ac.za

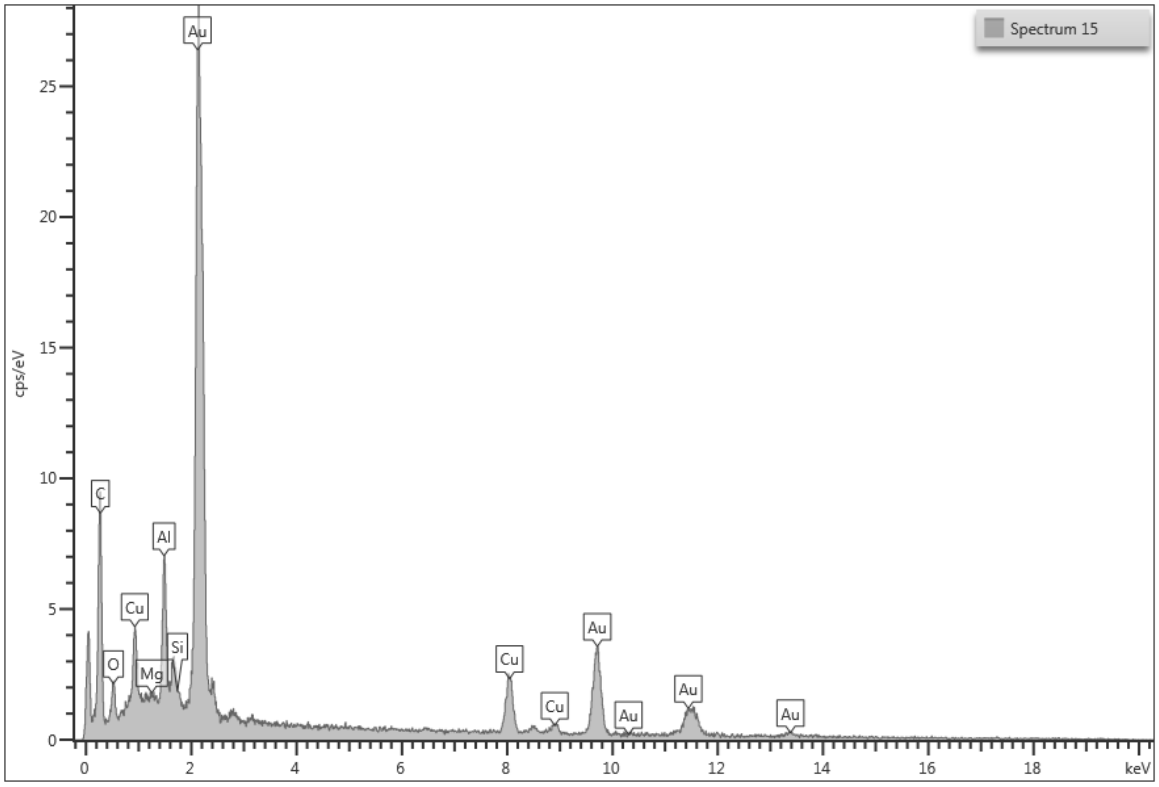

Figure 21a: Elemental mapping of chitosan capped GYY4137-AuNPs as per EDX Oxford Aztec software image.

UNIVERSITY of the
WESTERN CAPE

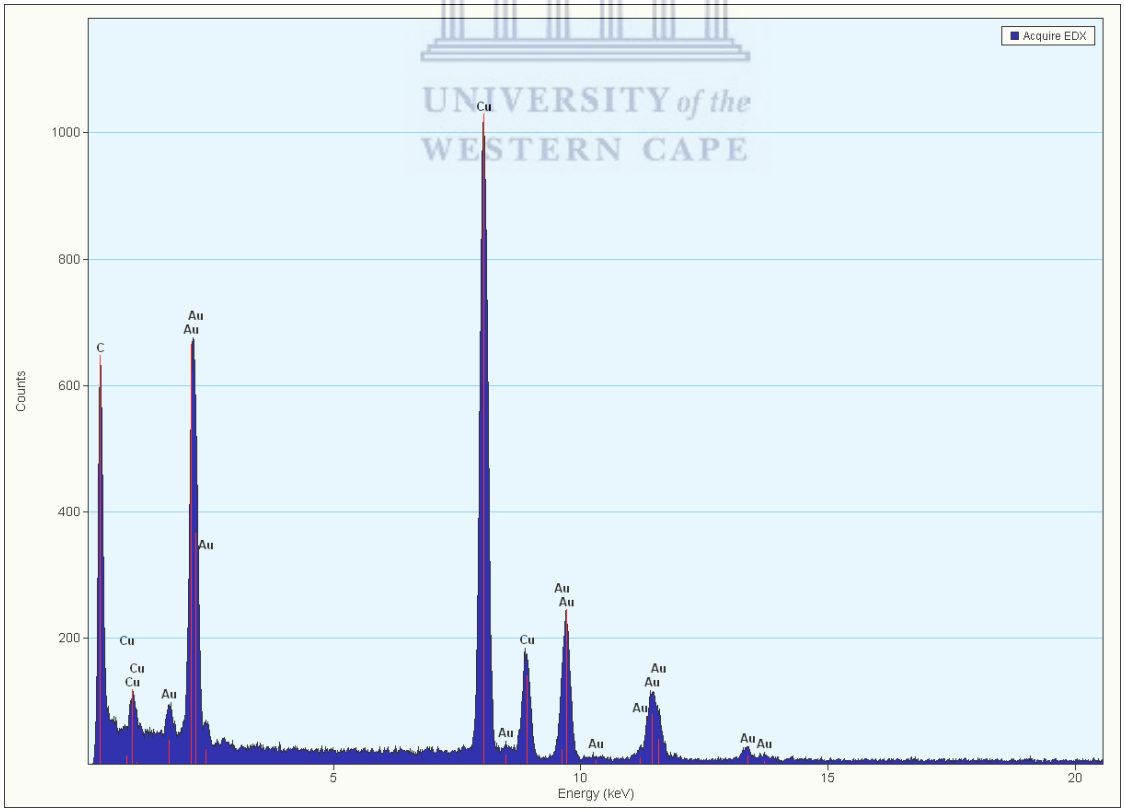

Figure 21b: Elemental mapping of serine-AuNPs as per EDX image.

https://etd.uwc.ac.za

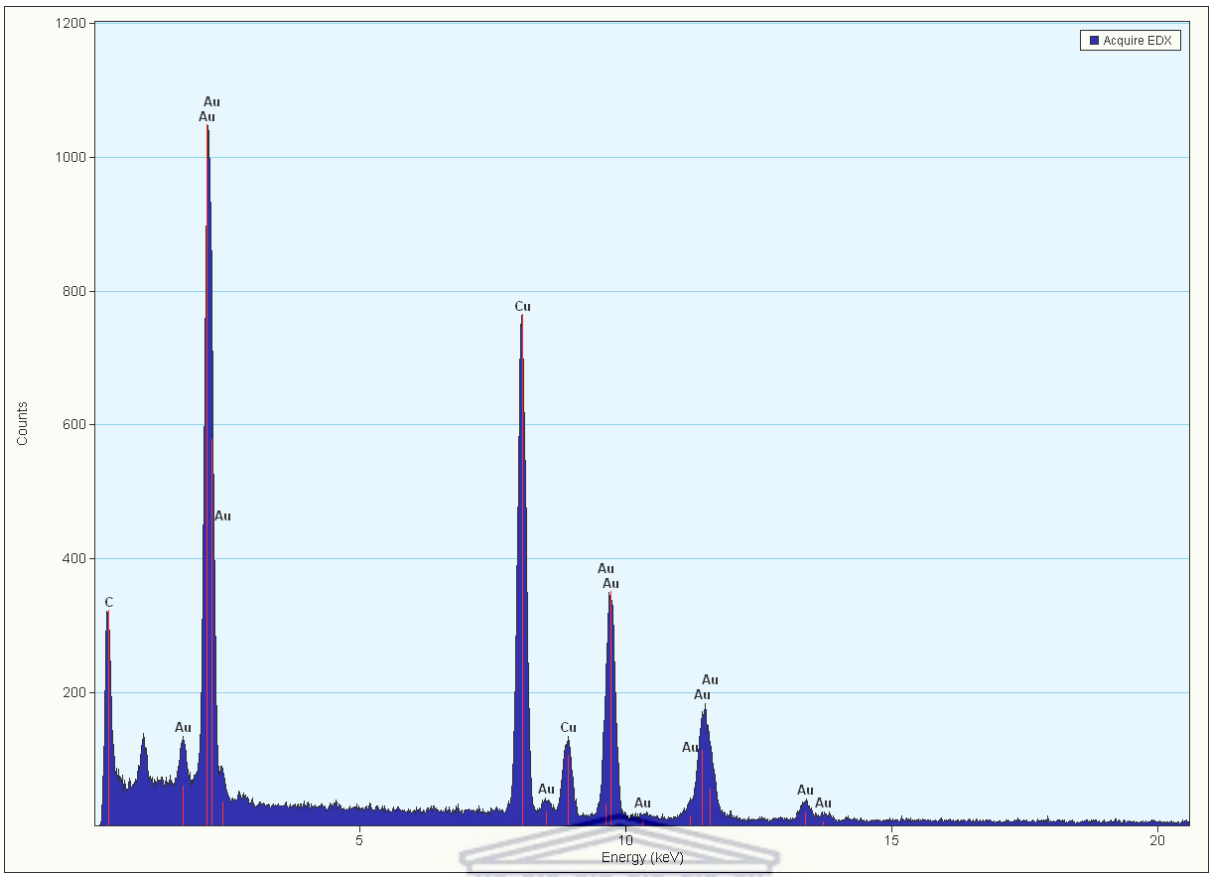

Figure 21c: L-threonine-AuNPs as per EDX image.

UNIVERSITY of the
WESTERN CAPE

4.3. References

1. Ashrafi A. (2011). Quantum Confinement: An Ultimate Physics of Nanostructures. In A. Umar (Ed.) Encyclopedia of Semiconductor Nanotechnology. (Chapter1). American Scientific.
2. Belahmar, A. and Chouiyakh, A. (2016). Investigation of Surface Plasmon Resonance and Optical Band Gap Energy in Gold/Silica Composite Films Prepared by RF-Sputtering. *Journal of Nanoscience and Technology*, 2(2), pp.81–84.
3. Csapó, E., Sebők, D., MakraiBabić, J., Šupljika, F., Bohus, G., Dékány, I., Kallay, N. and Preočanin, T. (2014). Surface and Structural Properties of Gold Nanoparticles and Their Biofunctionalized Derivatives in Aqueous Electrolytes Solution. *Journal of Dispersion Science and Technology*, 35(6), pp.815-825.
4. Gupta, S., Singh, S. and Singh, R. (2015). Synergistic Effect of Reductase and Keratinase for Facile Synthesis of Protein-Coated Gold Nanoparticles. *Journal of Microbiology and Biotechnology*, 25(5), pp.612-619.

https://etd.uwc.ac.za

5. Jain, P., Lee, K., El-Sayed, I. and El-Sayed, M. (2006). Calculated Absorption and Scattering Properties of Gold Nanoparticles of Different Size, Shape, and Composition: Applications in Biological Imaging and Biomedicine. *The Journal of Physical Chemistry B*, 110(14), pp.7238-7248.
6. Judy, J. D., Unrine, J. M., Rao, W., Wirick, S., and Bertsch, P. M. (2012). Bioavailability of gold nanomaterials to plants: importance of particle size and surface coating. *Environmental. Science and Technology*, 46, 8467–8474.
7. Keshvari, F., Bahram, M. and Farshid, A. (2015). Gold nanoparticles biofunctionalized (grafted) with chiral amino acids: a practical approach to determining the enantiomeric percentage of racemic mixtures. *Analytical Methods*, 7(11), pp.4560-4567.
8. Kadajji, V. and Betageri, G. (2011). Water Soluble Polymers for Pharmaceutical Applications. *Polymers*, 3(4), pp.1972-2009.
9. Rose, P., Dymock, B., and Moore, P. (2015). GYY4137, a Novel Water- Soluble, H_2S releasing molecule. *Methods of Enzymology*, 554, pp.143-161.
10. Składanowski, M., Wypij, M., Laskowski, D., Golińska, P., Dahm, H. and Rai, M. (2016). Silver and gold nanoparticles synthesized from Streptomyces sp. isolated from acid forest soil with special reference to its antibacterial activity against pathogens. Journal of Cluster Science, 28(1), pp.59-79.
11. Tantra, R., Schulze, P. and Quincey, P. (2010). Effect of nanoparticle concentration on zeta-potential measurement results and reproducibility. *Particuology*, 8(3), pp.279-285.
12. Tiede, K., Hassellöv, M., Breitbarth, E., Chaudhry, Q. and Boxall, A. (2009). Considerations for environmental fate and ecotoxicity testing to support environmental risk assessments for engineered nanoparticles. *Journal of Chromatography A*, 1216(3), pp.503-509.
13. Utdallas.edu. (2019). *INFRARED SPECTROSCOPY (IR): Theory and Interpretation of IR spectra*. [online] Available at: https://www.utdallas.edu/~scortes/ochem/OChem_Lab1/recit_notes/ir_presentation.pdf [Accessed 10 May. 2019].
14. Wangoo, N., Kaur, S., Bajaj, M., Jain, D. and Sharma, R. (2014). One pot, rapid and efficient synthesis of water dispersible gold nanoparticles using alpha-amino acids. *Nanotechnology*, 25(43), p.435608.
15. Zarabi, M., Arshadi, N., Farhangi, A. and Akbarzadeh, A. (2013). Preparation and Characterization of Gold Nanoparticles with Amino Acids, Examination of Their Stability. *Indian Journal of Clinical Biochemistry*, 29(3), pp.306-314

UNIVERSITY of the WESTERN CAPE
https://etd.uwc.ac.za

16. Zhu, Z., Wang, H., Yan, B., Zheng, H., Jiang, Y., Miranda, O., Rotello, V., Xing, B. and Vachet, R. (2012). Effect of Surface Charge on the Uptake and Distribution of Gold Nanoparticles in Four Plant Species. *Environmental Science & Technology*, 46(22), pp.12391-12398.

https://etd.uwc.ac.za

Chapter 5: Conclusions and Future Perspectives

This chapter presents the conclusion and future prospects on the synthesis and characterization of the novel GYY4137 nanoparticles.

5.1. Conclusions

The aim of this project was to synthesize GYY4137 gold nanoparticles (GYY4137-AuNPs), stabilize them using water-soluble polymers (poly ethylene glycol (PEG) and chitosan) and characterize with standard techniques such UV-Vis, HRTEM and FTIR among others compared to amino acid produced gold nanoparticles (serine and threonine). The uncapped GYY4137-AuNPs were relatively stable compared to stable serine and threonine-AuNPs. Stabilization with poly (ethylene) glycol was unsuccessful and interfered completely with chemical reduction of the synthesis procedure. The chitosan-achieved surface charge stability of + 47.8 mV in the GYY4137-AuNPs resulting in polydispersed icosahedron, spherical shaped gold nanoparticles compared to spherical shaped of serine-AuNPs that absorb at 550 nm. The chitosan capped GYY4137-AuNPs HRTEM resulted in 100 nm and 60 nm in STEM with some nanoparticles in the 20 nm. The hydrodynamic size of 375 nm also proved that the chitosan a polymer capped the GYY4137 AuNPs and their size increased. The chemical shifts in FTIR spectra also proved the successful encapsulation of GYY4137-AuNPs by chitosan. EDX showed the elemental composition showing presence of Au in the samples. The objectives of the study were achieved resulting in the chitosan capped GYY4137-AuNPs stable for more than 30 days. The chitosan encapsulation improved surface charge and reactivity of the gold nanoparticles to improve delivery of the hydrogen sulfide donor GYY4137 for later applications to plants.

UNIVERSITY of the
WESTERN CAPE

5.2. Future Perspectives

In the future, the stable chitosan capped GYY4137-AuNPs will be evaluated for their stability and safety in biological samples prior to application in plants or any other biological samples. Furthermore investigate the gold nanoparticle's uptake, bioaccumulation and transport into the biological samples.

https://etd.uwc.ac.za

Appendix 1: HRTEM structural shapes of chitosan capped GYY4137 nanoparticles

We have some of the interesting STEM images captured for the GYY4137-AuNPs

1.

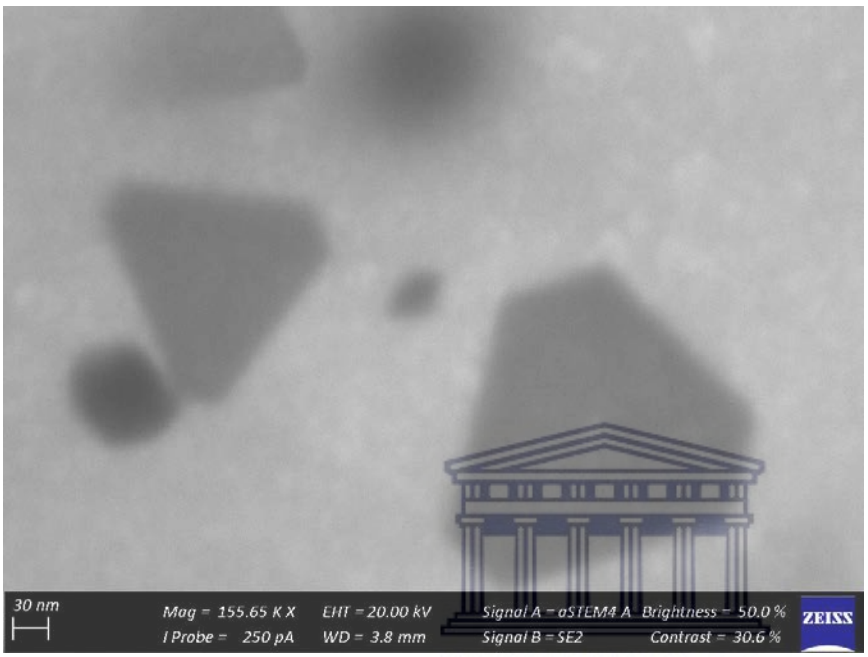

UNIVERSITY of the
WESTERN CAPE

2.

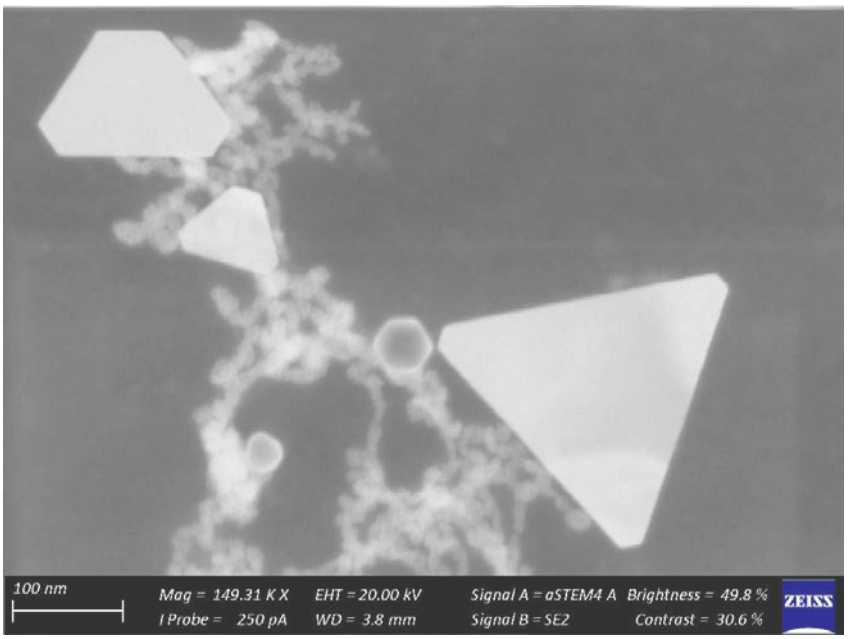

https://etd.uwc.ac.za

3.

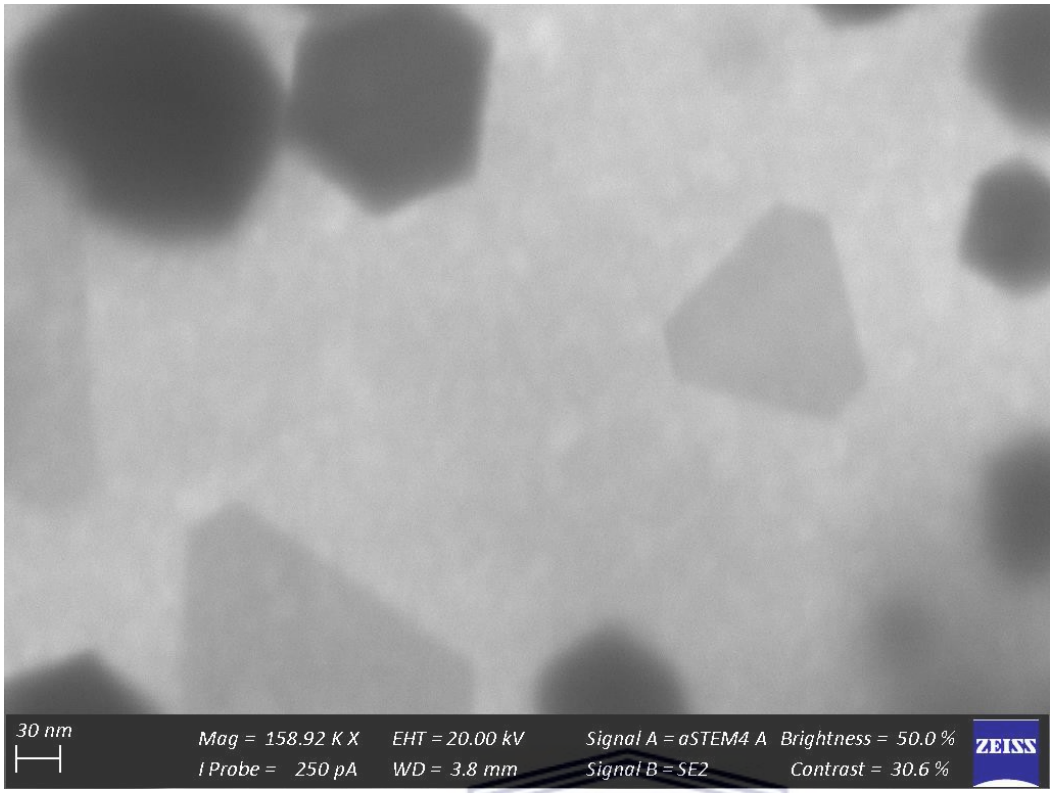

4.

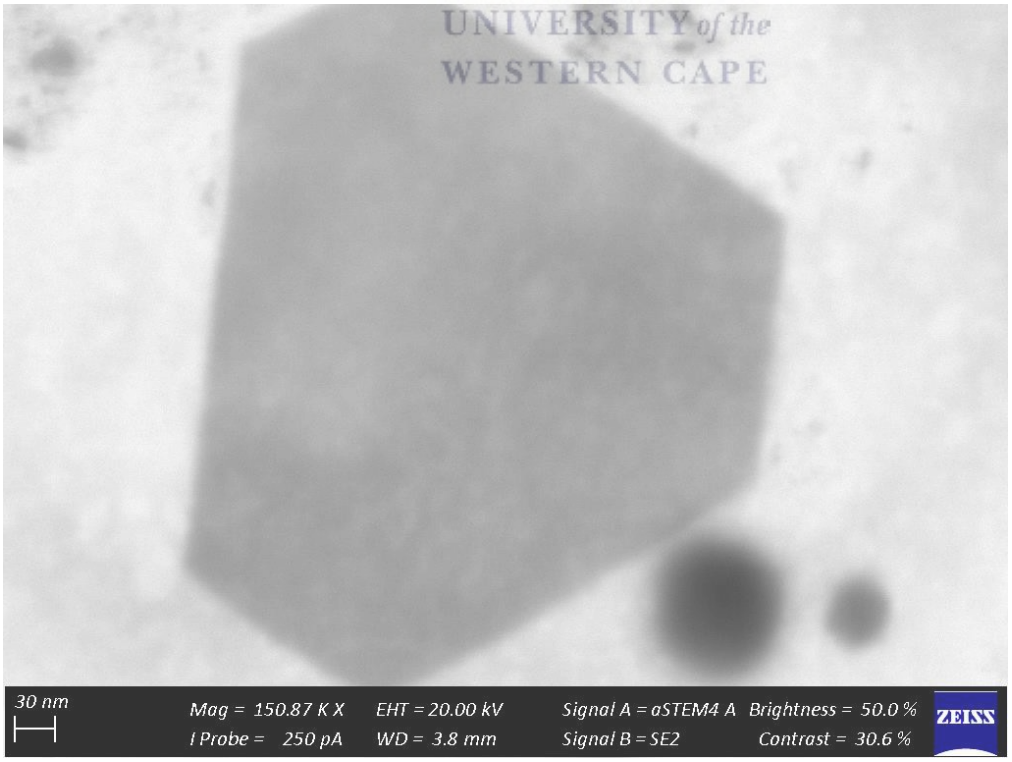

UNIVERSITY of the
WESTERN CAPE

https://etd.uwc.ac.za

5.

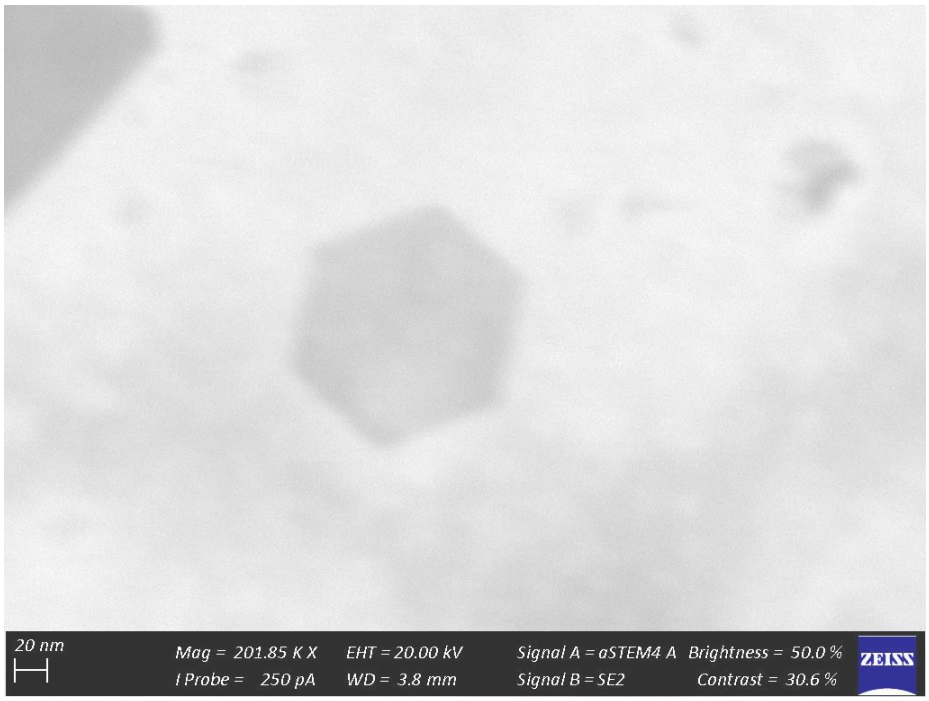

UNIVERSITY of the
WESTERN CAPE

https://etd.uwc.ac.za